CHAPTER 4

Results and discussion (part I): Materials characterization of potassium sodium niobate based tellurite glass-ceramics

In this chapter, materials characterization of transparent glasses and glass-ceramics containing ferroelectric potassium sodium niobate $(K_{0.5}Na_{0.5})NbO_3$ (KNN) crystals in a tellurite (TeO_2) glass system were studied. The samples were prepared via an incorporation method. The prepared glasses were subjected to heat treatment in order to grow the crystals inside glass matrix. The basic properties like physical, electrical, optical and microstructure have been carried out in this chapter. In the first section, the properties of 30KNN-70TeO_2 and 20KNN-80TeO_2 have been demonstrated. After that, the suitable glass was selected to dope with Er_2O_3 in order to study the effect of doping Er_2O_3 on glass properties, especially optical property. The study ensured that Er_2O_3 dopant has shown significant effect on the properties of glass-ceramics as described in section 4.2.

4.1 Characterization of KNN-TeO_2 glasses and glass-ceramics

The well prepared KNN single phase ceramic powders were mixed with TeO_2 in compositions of 30KNN-70TeO_2 and 20KNN-80TeO_2, owing to previous studied which demonstrated the optimize composition ratio of TeO_2 in forming transparent glass was about 70 mol% [104]. The weight percent of 30KNN-70TeO_2 and 20KNN-80TeO_2 glasses are already calculated and showed in table 3.3. Fig. 4.1 showed the appearance of as-received glass (30KNN-70TeO_2) which is melted at 1000ºC, 900ºC and 800ºC for 15, 30 and 60 minutes, respectively.

Naturally, TeO_2 has very low meting point of about 732 ºC. The higher melting temperature of about 900 ºC may raise the degree of crystallization in these glasses, resulted in the decrease of transparency of glass as seen in the Fig. 4.1.

a) 1000ºC for 15 min. **b)** 900ºC for 15 min.

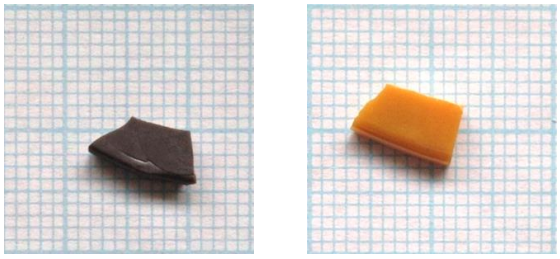

c) 800ºC for 15 min**.** **d)** 800ºC for 30 min. **e)** 800ºC for 60 min.

Figure 4.1 Appearance of as-received glasses (30KNN-70TeO_2) melted at various temperatures and times; **(a)** 1000ºC for 15 minutes, **(b)** 900ºC for 15 minutes, **(c)** 800ºC for 15 minutes, **(d)** 800ºC for 30 minutes and **(e)** 800ºC for 60 minutes.

Glass compositions of 1000ºC for 15 minutes (a) and 900ºC for 15 minutes (b) were opaque due to crystallization, and similar result also found in a longer dwell time of 60 min sample. The longer dwell time may lead to increase the crystal grow rate with a larger size, and causing the scattering of light. From Fig. 4.1, almost of as-received glasses were orange in color except that of the glass melted at 1000ºC for 15 minutes which was black, and all samples have low mechanical strength, as they are brittle and difficult to handle. Thus, the annealing process was taken into consideration by choosing from their thermal behavior measured from DTA analysis. This process was performed to prevent glass from crack and shatter by relieved internal stress, as known as thermal shock. The quenched glass was immediately annealed in another electric furnace at 300ºC for 6 hours to release their stress. Then, annealed glass was subjected to heat treatment (HT) in order to grow the KNN crystal inside a glass matrix.

In this studies, the condition for melting appropriate transparent glasses has been chosen as 800ºC for 15 minutes. To analyze the glass and glass-ceramic properties, various techniques were employed. XRD and SEM techniques were used to investigate the phase

composition and to observe the microstructure of the glass and glass-ceramic samples. The room temperature dielectric constant (ε_r) and dielectric loss (tanδ) of the glass-ceramics measured at various frequencies and temperatures were measured. Finally, the transmission and refractive index values were investigated.

4.1.1 Thermal behavior determination

Transparent KNN glasses were obtained after melting and quenching of KNN and TeO_2 powder with weight ratio 30:70 and 20:80 mol% at 800ºC for 15 minutes. As-received glasses were orange in color and had low mechanical strength as shown in Fig. 4.1. Thus, annealing was employed to reduce stress in the quenched glass which measured from the differential thermal analysis or DTA. Annealing temperature for the glass was decided from the DTA traces of the two glasses and was chosen near their glass transition (T_g) points. DTA traces are shown in Fig. 4.2.

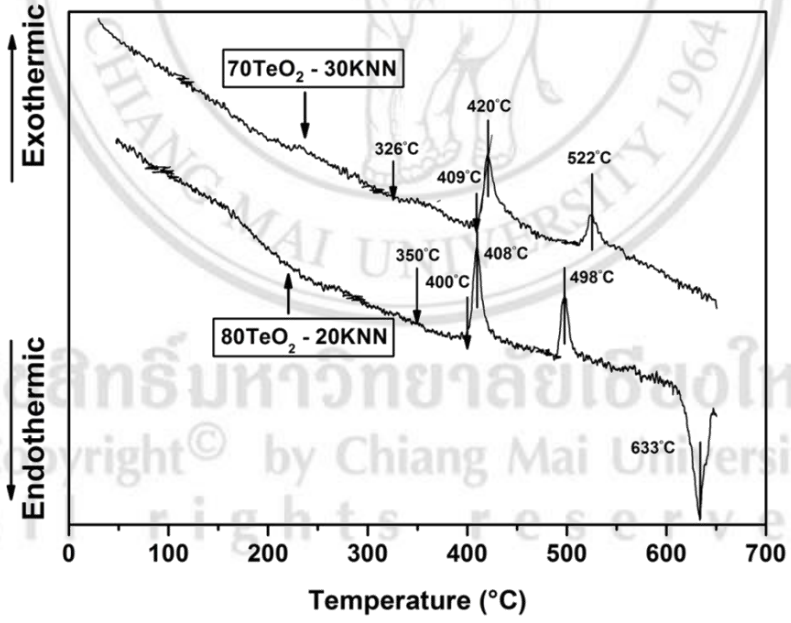

Figure 4.2 Thermal analysis (DTA) of KNN-TeO_2 glasses which were melted at 900ºC for 15 minutes and quenched between stainless steel plates at room temperature.

Fig. 4.2 show that 30KNN-70TeO_2 and 20KNN-80TeO_2 glasses have T_g around 325-350ºC. Crystallization temperatures (T_c) of the two glass compositions were different. For the 30KNN-70TeO_2 glass, T_{c1} and T_{c2} at

420°C and 522°C were observed while for 20KNN- 80TeO_2 glass, T_{c1} and T_{c2} were at 408°C and 498°C. Small differences between these thermal parameters may arise from the difference in TeO_2 concentration as shown in Fig. 4.2 and Table 4.1. The slightly increase of glass transition temperature with decreasing TeO_2 content is similar to that found in $TeO_2 \cdot LiNbO_3$ system of previous work done by Shankar and Varma [105]. In 20KNN-80TeO_2, the DTA trace also shows melting point (T_m) at 633°C. The T_m point can be used for estimate the glass forming ability (K_g) by using the relation below.

$$Kg = \frac{T_c - T_g}{T_m - T_c} \tag{4.1}$$

Here, the tendency of the ability in forming glass or K_g of 20KNN- 80TeO_2 is very low (K_g = 0.2578), which mean these glass compositions showed high tendency to devitrify. From Table 4.1, ΔT value is the thermal glass stability factor which is suitable for estimate the tendency of crystallization in glass. The ΔT value can be calculated from relation.

$$\Delta T = T_{c1(onset)} - T_g \tag{4.2}$$

This value is used to define the stability and usability of glass. The appropriate ΔT value should be more than 100°C for making a thick bulk glass. However, the observed low stability in this sample indicates that this glass composition is close to the boundaries of the glass formation range. Moreover, it may be assumed by considering the difference between these values of each glass that the 30KNN-70TeO_2 (ΔT ≈ 83°C) is more stable than that of the 20KNN-80TeO_2 (ΔT ≈ 56°C). This result was similar to that of Raouf A.H. El-Mallawany's review in 2001 [3]. They reported the thermal property of TeO_2 based glasses containing ferroelectric like $KNbO_3$, $LiTaO_3$, etc. The glass composition of 10$KNbO_3$-90TeO_2 showed glass stability of about 51.

Table 4.1 Thermal profile data of 2 glass compositions from DTA measurement.

Composition (mol%)	Glass Transition (°C)					
	T_g	$T_{c\ (onset)}$	T_{c1}	T_{c2}	ΔT	K_g
30KNN-70TeO_2	326	409	420	522	83	-
20KNN- 80TeO_2	350	400	408	498	50	0.2578

The heat treatment process was employed in order to crystallize KNN crystals in the glass matrix with the desired crystal size. The glasses were subject to heat treatment schedules at 325°C, 350°C and at their T_{c1} and T_{c2}. The heat treatment near T_g in the range of 325- 350°C was performed to achieve transparent glass-ceramics, while the heat treatment at T_{c1} and T_{c2} was for checking formation of crystal phases at their crystallization temperatures. The appearances of all glass-ceramics are displayed in Fig. 4.3 and Fig. 4.4.

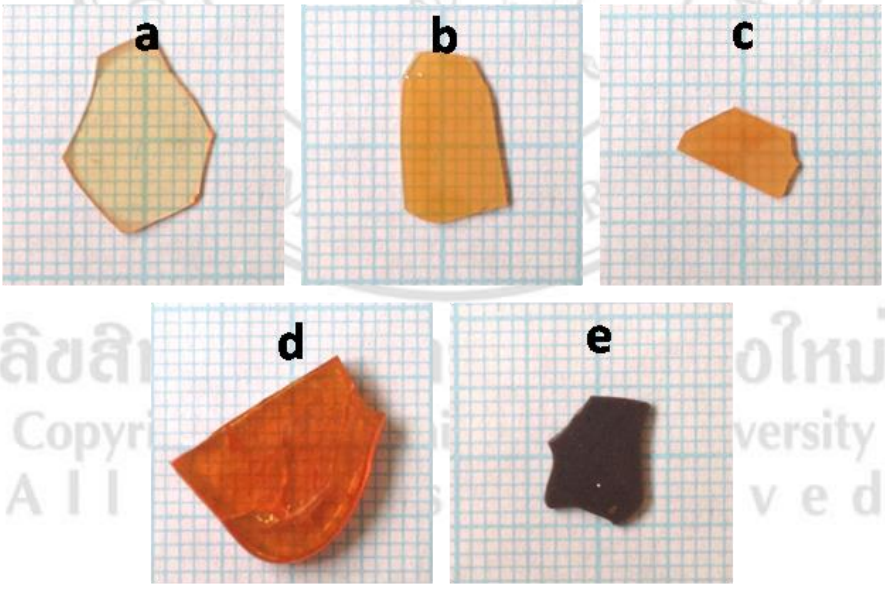

Figure 4.3 Physical appearances of 30KNN- 70TeO_2 glass-ceramics after various heat treatment (HT) temperatures **a)** annealed glass at 300°C, **b)** HT at 325°C, **c)** HT at 350°C, **d)** HT at 420°C and **e)** HT at 522°C**.**

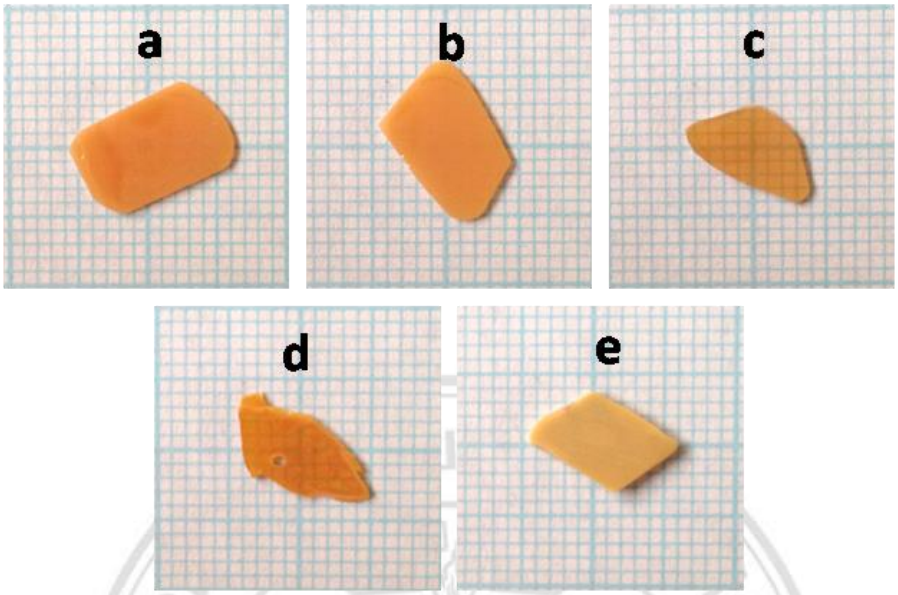

Figure 4.4 Physical appearances of 20KNN- 80TeO_2 glass-ceramics at various heat treatment temperatures (HT) **a)** annealed glass at 300°C **b)** HT at 325°C, **c)** HT at 350°C, **d)** HT at 408°C and **e)** HT at 498°C**.**

4.1.2 Densification investigation

Densities as a function of HT temperature of the prepared glass-ceramics are shown in Fig. 4.5. The density trend was found to increase with heat treatment temperature because of the growth of crystals crystalline decreased the volume of crystallization as shown in SEM micrographs (Topic 4.1.4).

Higher values were found in the series of 20KNN - 80TeO_2 glass-ceramics. This may be due to the lower value of density of KNN (4.64 g/cm^3) than that of TeO_2 (5.67 g/cm^3) [Please see Appendix A and B]. Thus, this high content of TeO_2 was assumed to raise the density of 80 mol% of TeO_2 glass composition. However, heat treatment time is also play a significant role in controlling the crystallization size. Many previous works found that dwell time could raise the density values as review in [3], which mean the longer heat treated time, the higher density of the glass-ceramics can be achieved. This may from the longer time allows the crystal to grow homogeneously. Thus, the effect of dwell time should be put in the further study.

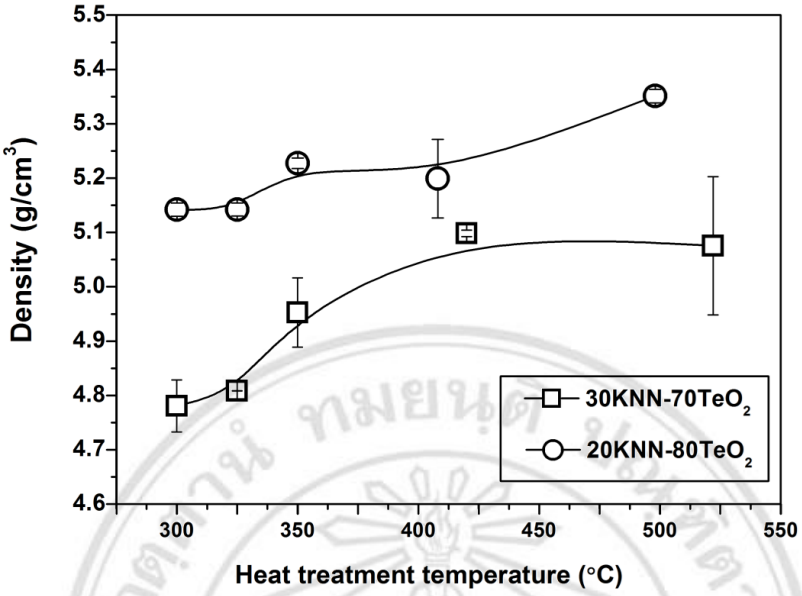

Figure 4.5 Density of glass and glass-ceramics comparing with HT temperature.

4.1.3 Structural formation

1) Phase composition studied by XRD

The XRD results in Fig. 4.6 of the heat treated glass-ceramics revealed that KNN; $(K_{0.5}Na_{0.5})NbO_3$ was not retained by the incorporation method. This may be due to the very low viscosity of telluride glasses at their melting temperatures, giving rise to compositional fluctuation in these glasses [106-108]. However, the heat treatment temperature plays an important role in controlling the crystal phase in these glass-ceramics. At low temperature from 300^{o}C to 350^{o}C, the resulting glass-ceramics for both compositions, contained similar crystal phase, which may be identified as the typical cubic structure of (K,Na)NbO_3 with random variation of K and Na ions in the A-site of the unit cell. This result is consistent with the work done by Jeong et al. [109] who studied the glasses of xK_2O-(14-x)Na_2O-14Nb_2O_5-72TeO_2 where x = 0∼12 mol%. For annealed glass at 300^{o}C, the glass-ceramics sample for the 30KNN-70TeO_2 glass series exhibited slightly amorphous patterns with a trace at crystalline peaks of the same cubic (K,Na)NbO_3 (∗) phase.

For the 20KNN-80TeO_2 series, the crystalline peaks of the cubic phase were more revealed, indicating a higher degree of crystallinity. This is more evidence of greater glass stability of the 30KNN-70TeO_2 glass series over that of the 20KNN-80TeO_2, confirming the DTA result as mentioned before. Moreover, this also affirms the previous work done by Jeong et al. [109].

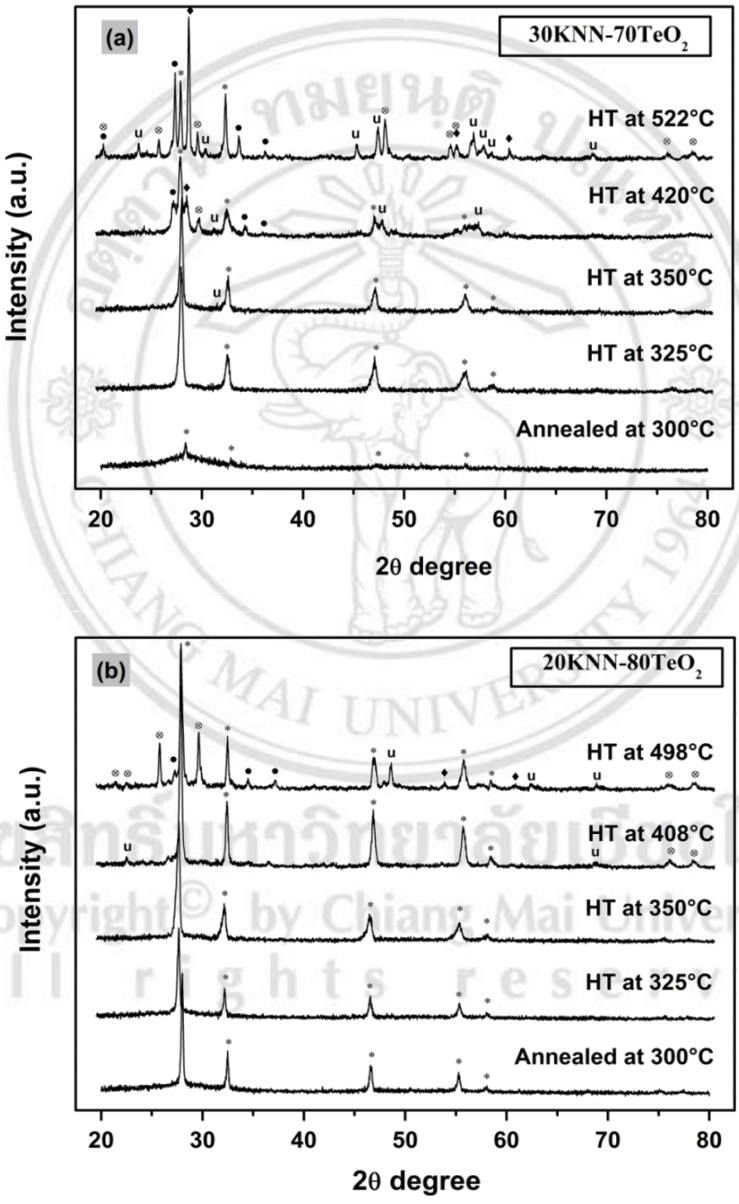

Figure 4.6 XRD patterns of two series of glass-ceramics 30KNN-70TeO_2 **(a)** and 20KNN-80TeO_2 **(b)** after various HT temperatures. (●=$KNbTeO_6$ peaks, ⊗=α-TeO_2 peaks, ∗=KNN solid solution, ♦=$Na_2Nb_4O_{11}$ peaks and **u**=unidentified phases)

The glass-ceramics heat treated at T_{c1} and T_{c2} for each glass series are also illustrated in Fig. 4.6. It can be seen that the 30KNN-70TeO_2 glass ceramic with HT = 420°C (T_{c1}) contained two other phases apart from the cubic (K,Na)NbO_3 phase (∗), which may be identified as $KNbTeO_6$ (●) and TeO_2 (⊗), while that of the 20KNN-80TeO_2 glass ceramic had no trace of any other phase apart from the (K,Na)NbO_3. At T_{c2} for both glass series, the additional $Na_2Nb_4O_{11}$ (♦) phase was clearly revealed, together with two phases of $KNbTeO_6$ (●) and TeO_2 (⊗). However, the amount of $KNbTeO_6$ phase of the 30KNN-70TeO_2 (HT at T_{c2} = 522°C) was greater than that found in the 20KNN-80TeO2 (HT at T_{c2} = 498°C). From the full width at half maximum (FWHM) values of the most intense diffraction peak detected from XRD patterns, the average crystallite sizes (diameter, *d*) were calculated by conventional procedure using the Scherrer's equation [97].

$$d = \frac{0.9\lambda}{\beta \cos\theta} \tag{4.3}$$

where, λ is the wavelength of X-ray radiation (CuKα = 1.5406 A°), β is the FWHM of the reflection peak that has the maximum intensity in the diffraction pattern. The diffraction peak located at 2θ = 28° (2θ = maximum intensity peak) has been considered for this estimation. The calculated average crystallite sizes are summarized in Table 2. It can be seen that the crystallite size analyzed from XRD increased with increasing heat treatment temperature. The crystallite sizes are varied after different heat treatment glasses because of the occurrence of new phases at high heat treatment temperatures.

Table 4.2 The calculated average crystallite sizes in two glass compositions.

Condition	Treatment temperature (°C)	Crystallite size (nm)
30KNN- 70TeO_2	300	35
	325	62
	350	31
	420 (T_{c1})	35
	522 (T_{c2})	46
20KNN- 80TeO_2	300	46
	325	111
	350	69
	408 (T_{c1})	111
	498 (T_{c2})	62

2) Phase formation studied by FTIR

FTIR studied in Fig. 4.7 exhibited broad absorption bands, especially in 80KNN-20TeO_2 glass series. From micrograph can be assumed that glass-ceramics in composition of 80KNN-20TeO_2 had lower KNN crystallinity than 70KNN-30TeO_2. The fused glass showed broad peak ranged from 400-800 cm^{-1}. This indicated that there are some disorders in the anionic network. Previous studies on telluride glass and niobium telluride glasses [110-112] have shown the symmetric and the anti-symmetric stretching modes. From 80KNN-20TeO_2 glass, the band at 600‑650cm^{-1} is attributed to TeO_4 tbp, which moved to higher frequency a little when increasing heat treatment temperature. The band at 730-760 cm^{-1} is attributed to TeO_3 tp, as same as in Raman spectra. Further, it is interesting to note that in this system the magnitude of stretching vibrational mode arising from non-bridging oxygen units belonging to TeO_3 trigonal pyramids (730 cm^{-1}) is at lowest and that of connecting bridging bonds of TeO_4 bi-pyramides (680 cm^{-1} and 595 cm^{-1}) is at highest. This is considered to be good indication of stability or resistant to devitrification. However, FTIR micrograph of 2 glass series exhibited the Nb-O bonding, which was occurred in several

pattern. The wide band of about 340-900 cm^{-1} with highest peak at around 520 cm^{-1} attributed to Nb-O bonds in the [NbO_6] octahedral. The small FTIR peak at around 890 cm^{-1} is also attributed to NbO_4 tetrahedra which less intense found in these glass compositions.

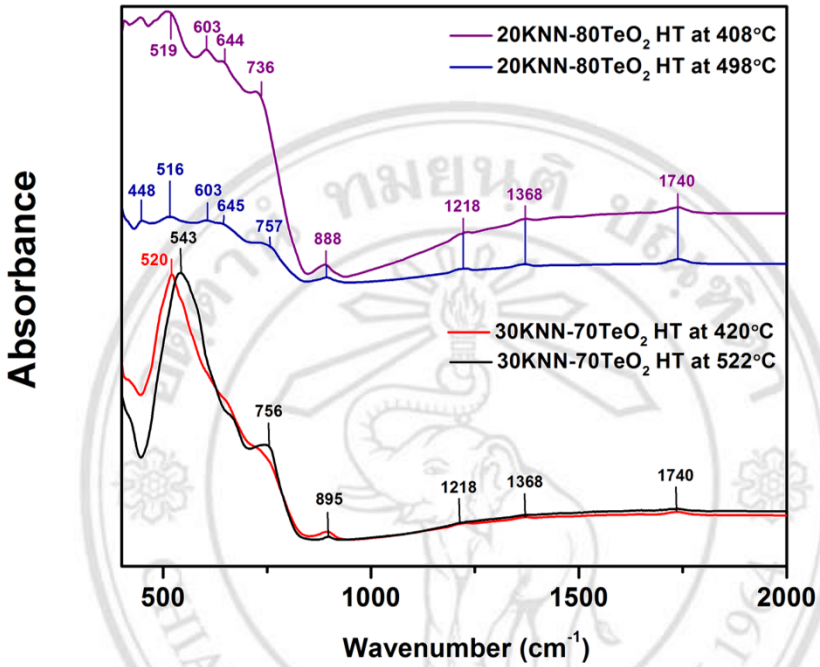

Figure 4.7 FTIR patterns of 20KNN-80TeO_2 and 30KNN-70TeO_2 systems after heat treatment at T_{c1} and T_{c2}.

4.1.4 Microstructure observation

SEM micrographs and EDS analysis of cross-sectional morphology of 30KNN-70TeO_2 and 20KNN-80TeO_2 glasses and glass-ceramics heat-treated at 350°C, T_{c1} and T_{c2} for 4 hours were illustrated in Fig. 4.8 and Fig. 4.9, respectively. All micrographs were taken at the same magnification. There are no clearly crystals found in samples with heat treated below 350°C. This might become from the small crystal with nanometer in size was occurred in glass matrix. The confirmation of the nanometer crystals size was aforementioned in Topic 4.1.3. A small peak of XRD patterns in samples heat treated below 350°C establish the small crystals inside glass matrix had occurred.

Microstructure of glass-ceramics 30KNN-70TeO_2 heat treated at 350°C was nearly amorphous phase which showed small bulks of crystals dispersed in glass-ceramic samples (Fig. 4.8(a)). This result was different from sample of 20KNN-80TeO_2, which the heat treated at 350°C samples showed crystallization homogeneously dispersed all over glass-ceramic area (Fig. 4.9(a)). Then, after heat up to T_{c1} and T_{c2}, the crystals were growth respectively. It can be clearly seen from the micrographs that, some large crystals (bright phase) were inhomogeneously dispersed in the glass matrices.

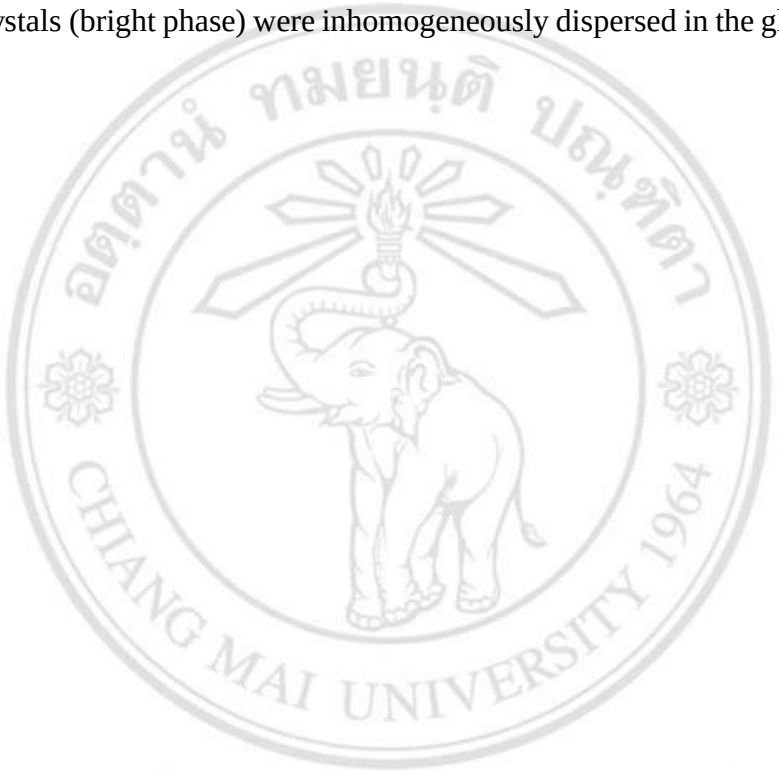

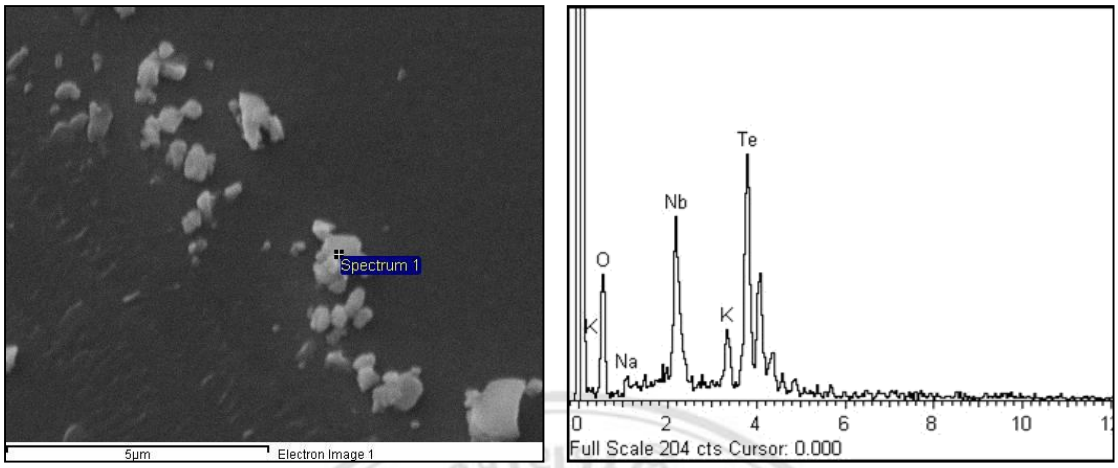

(a) 30KNN- 70TeO_2 HT at 350°C for 4 hour

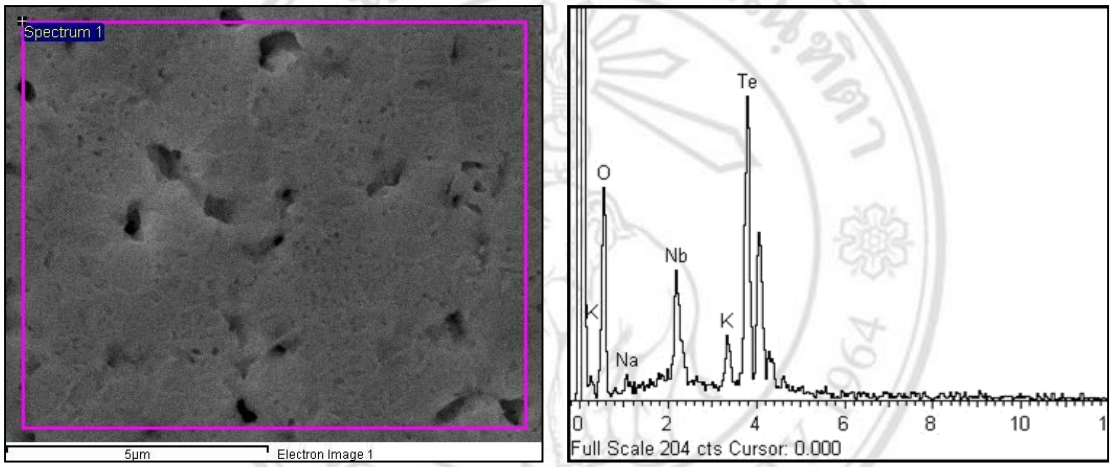

(b) 30KNN- 70TeO_2 HT at 420°C for 4 hour

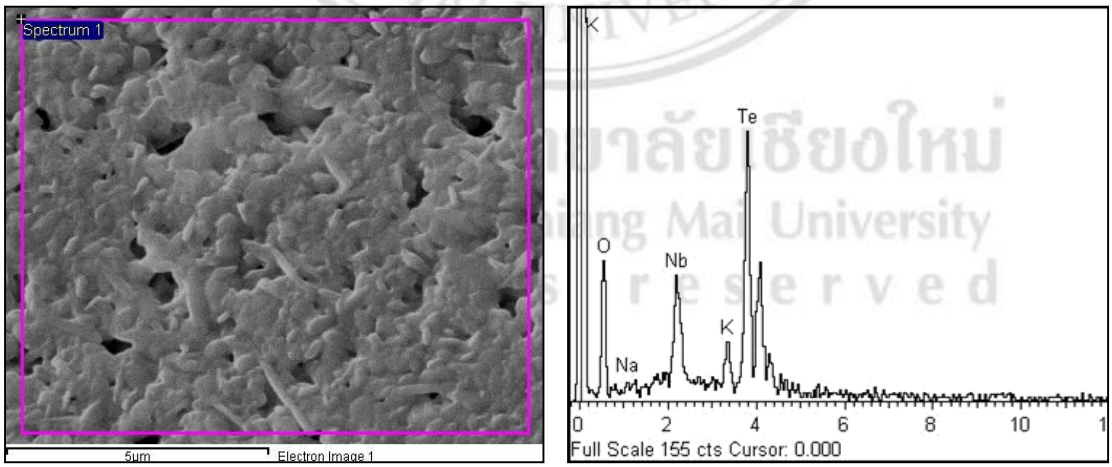

(c) 30KNN- 70TeO_2 HT at 522°C for 4 hour

Figure 4.8 SEM-EDS of 30KNN- 70TeO_2 glass-ceramics heat treated at different temperatures.

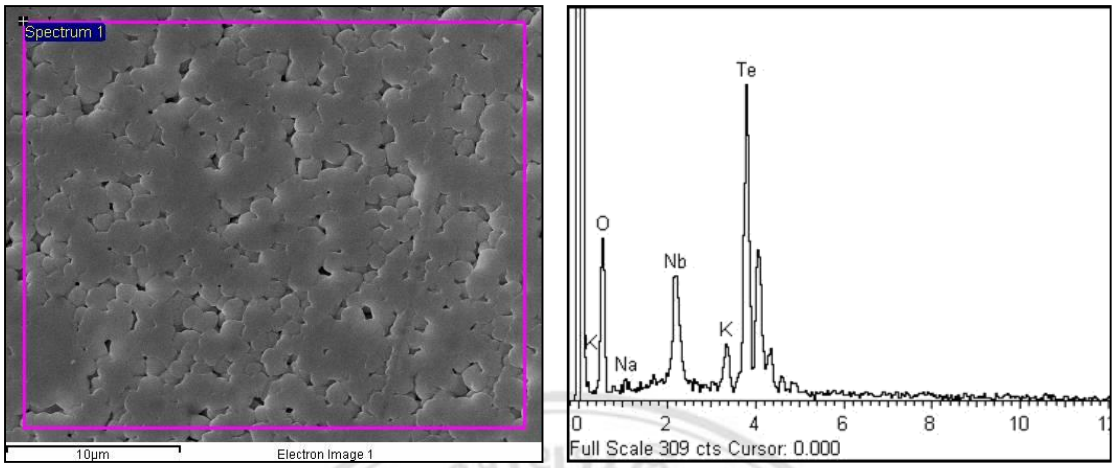

(a) 20KNN- 80TeO_2 HT at 350°C for 4 hour

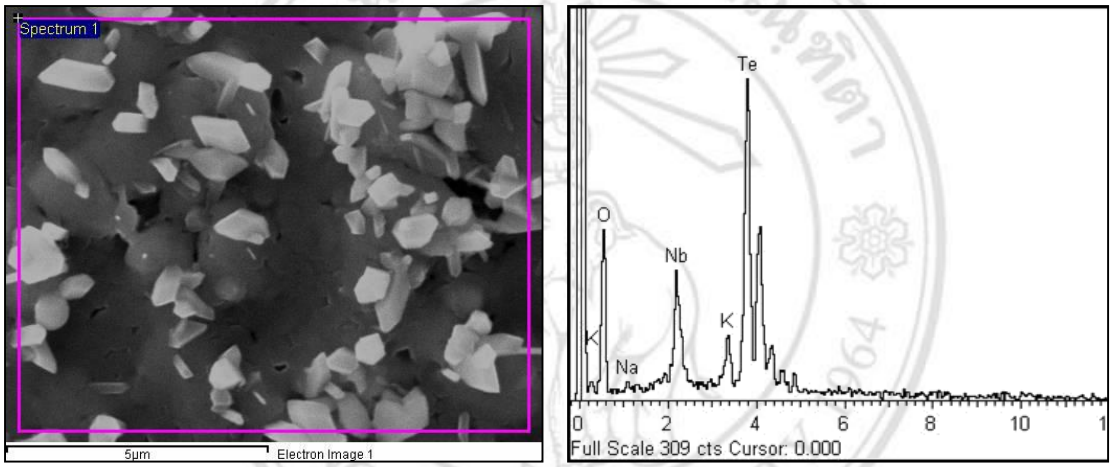

(b) 20KNN- 80TeO_2 HT at 408°C for 4 hour

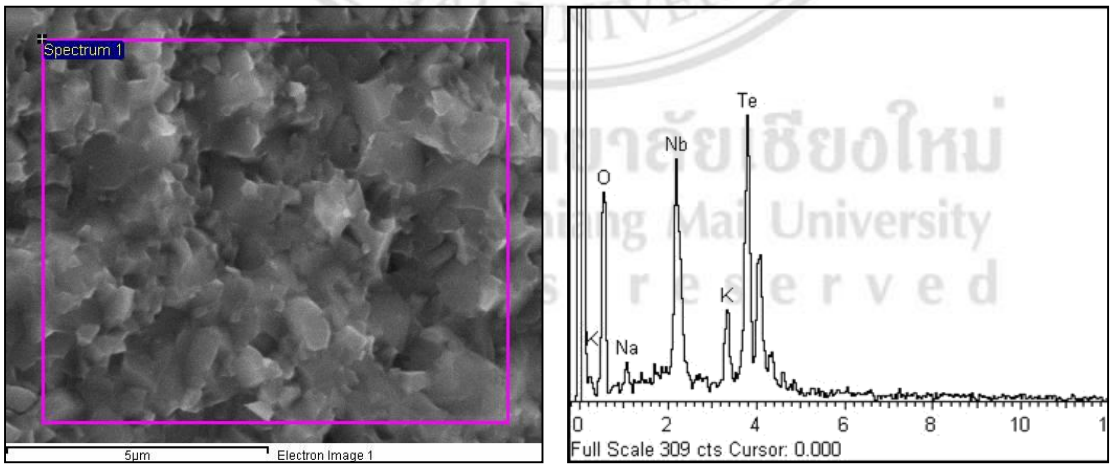

(c) 20KNN- 80TeO_2 HT at 498°C for 4 hour

Figure 4.9 SEM-EDS of 20KNN- 80TeO_2 glass-ceramics heat treated at different temperatures.

4.1.5 Electrical property

1) Dielectric constant at room temperature

In Fig. 4.10 shows the dielectric properties of the heat treated glass-ceramics at various temperatures. The maximum dielectric constant was found in 30KNN- 70TeO_2 glass-ceramic heat treated at T_{c2}, which was as high as 650 at 1 kHz and the dielectric loss was rather low about 0.02. It can be seen that the dielectric constant increased with increasing heat treatment temperature. The overall dielectric values of both glass-ceramics indicate that the higher amount of KNN addition in such a series of 30KNN- 70TeO_2 glass-ceramics could improve their dielectric properties.

2) Dielectric constant at different temperature

From Fig. 4.11 to 4.14, the dielectric constant and lose of glass-ceramics heat treated at T_{c1} and T_{c2} showed similar trend. After increasing heat treatment temperature, the dielectrics constant increased as well as dielectric losses. The highest dielectric was found in temperature around 400°C due to the change of microstructure from tetragonal to cubic structure. Besides, the increasing of heat treatment temperature, however, with increasing frequency, the dielectric constant values decreased. Moreover, it can be clearly seen that the more the TeO_2 content is in the glass-ceramic samples, the lower the dielectric constant value becomes.

(a)

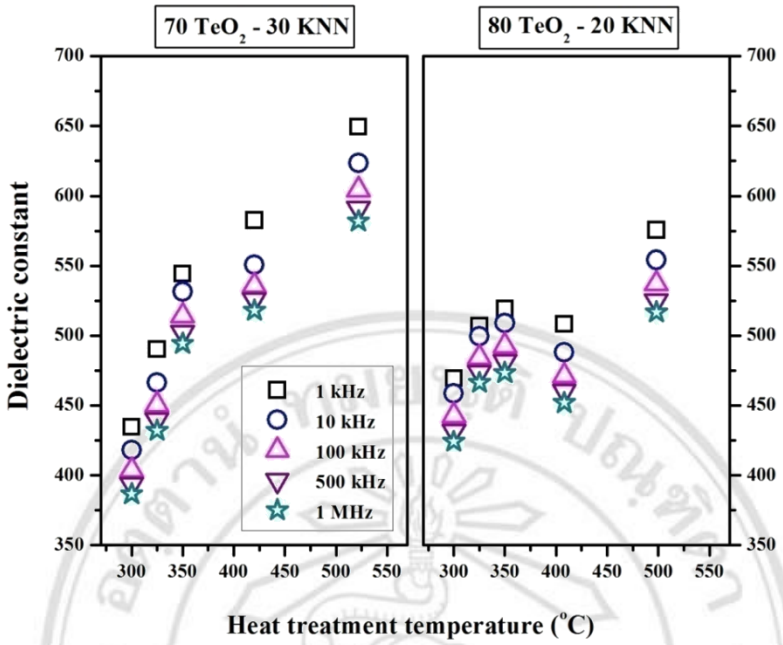

(b)

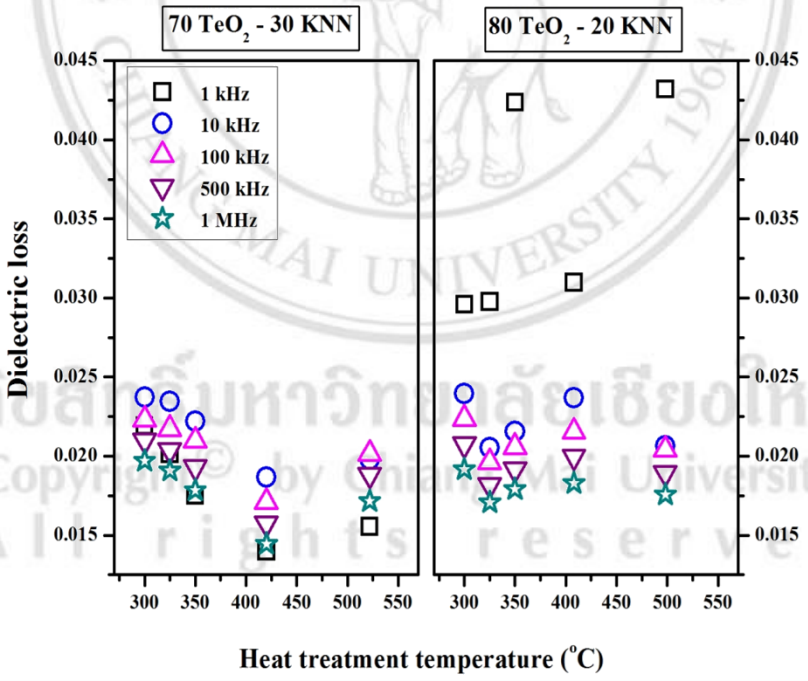

Figure 4.10 Dielectric constant **(a)** and dielectric loss **(b)** of two series of glass-ceramics at various HT temperatures and frequencies.

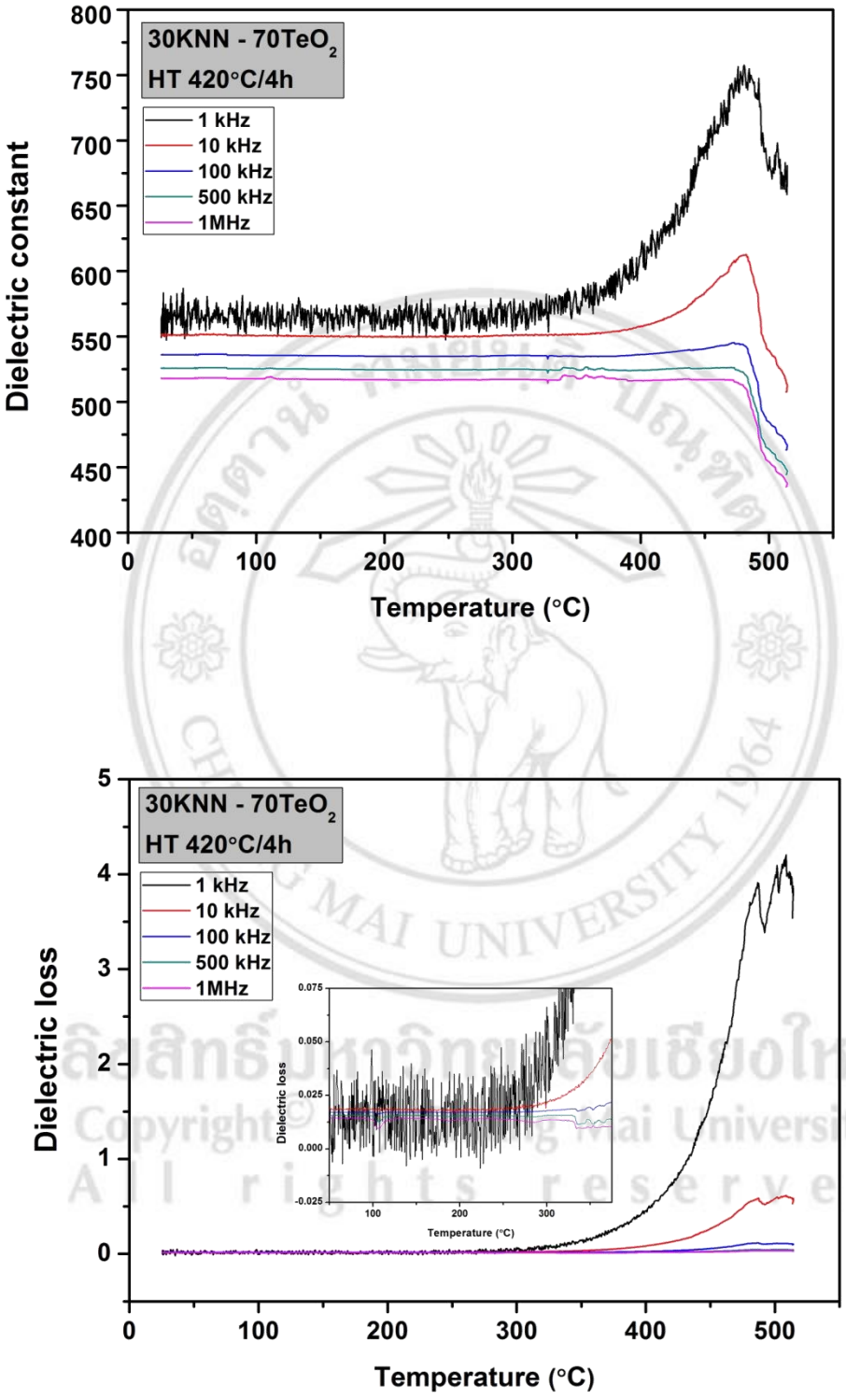

Figure 4.11 Dielectric constant and loss of glass-ceramics 30KNN-70TeO_2 heat treated at 420°C (T_{c1}) for 4 hours.

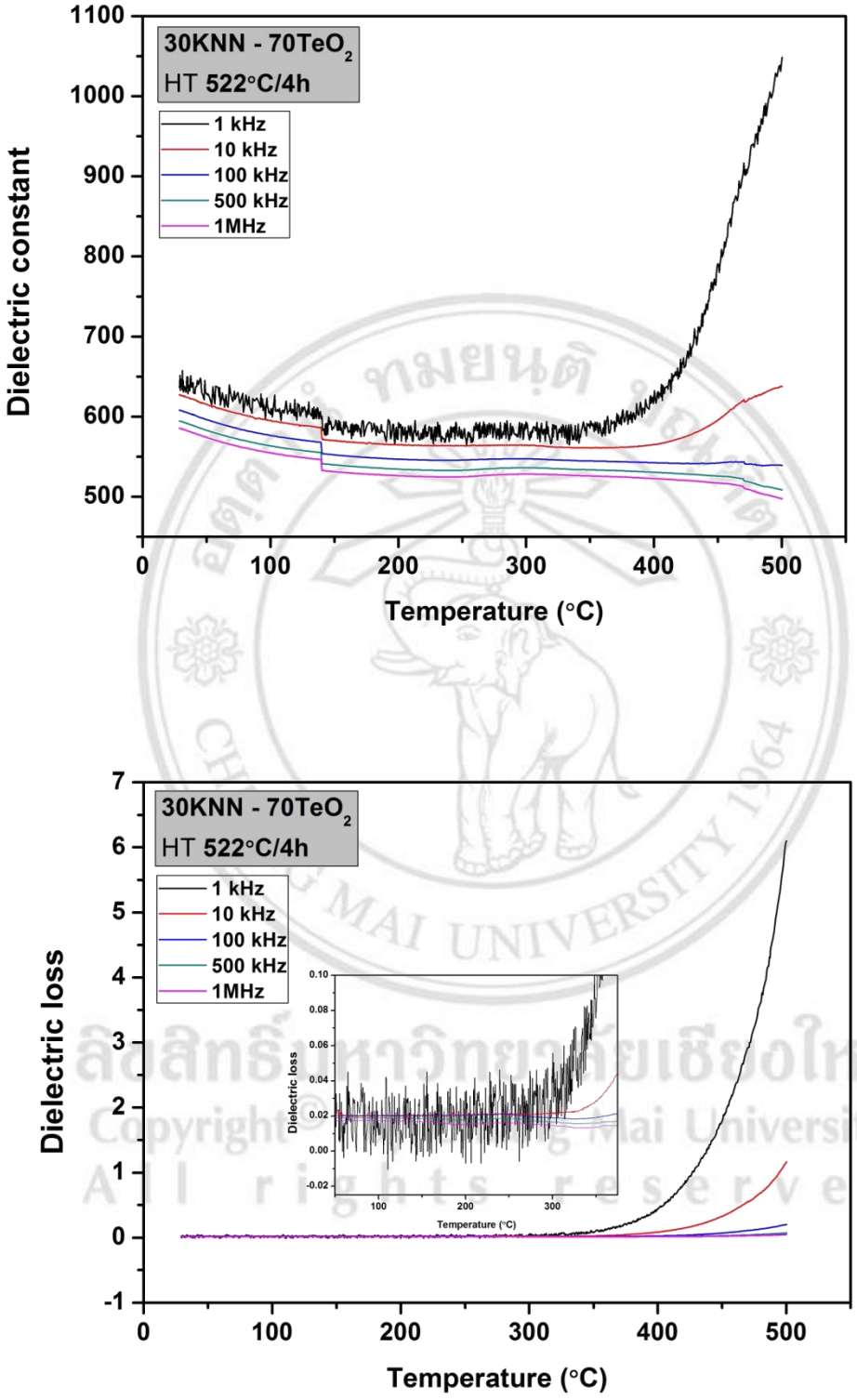

Figure 4.12 Dielectric constant and loss of glass-ceramics 30KNN-70TeO_2 heat treated at 522°C (T_{c2}) for 4 hours.

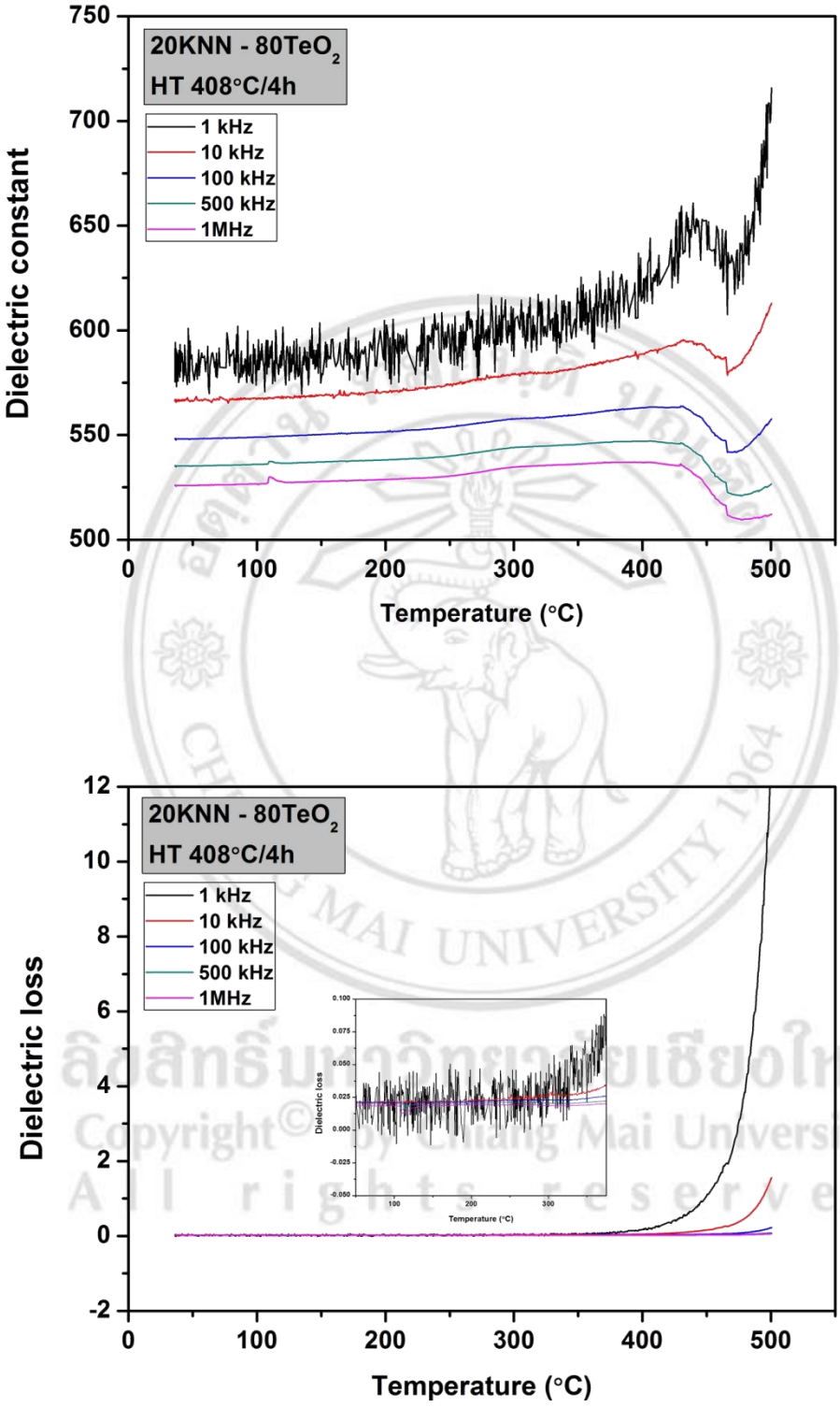

Figure 4.13 Dielectric constant and loss of glass-ceramics 20KNN-80TeO_2 heat treated at 408°C (T_{c1}) for 4 hours.

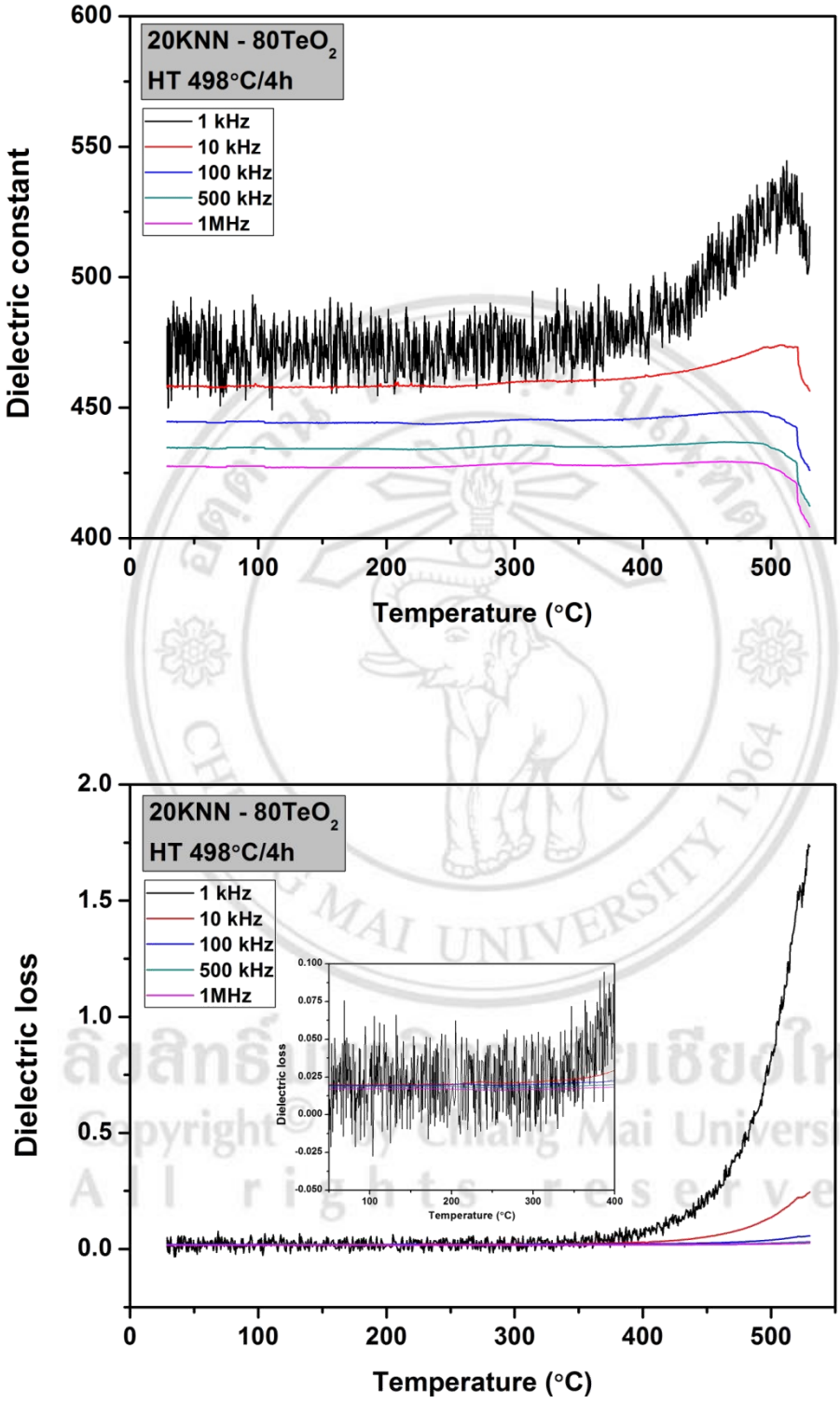

Figure 4.14 Dielectric constant and loss of glass-ceramics 20KNN-80TeO_2 heat treated at 498°C (T_{c2}) for 4 hours.

4.1.6 Optical property

1) Transmittance percentage

Fig. 4.15, shows optical transmission spectra of the quenched and heat treated samples of the 30KNN-70$TeO_2$and 20KNN-80TeO_2 glass-ceramics. All optical transmission spectra were recorded at room temperature. The percent transmission of all glass-ceramics tends to decrease with increasing HT temperature. The low transmission in glass-ceramics of 20KNN-80TeO_2 series heat treated at 300-325 ^oC confirms the appearance of glass-ceramics as shown in Fig. 4.3 and 4.4, having low transparency. The 30KNN-70TeO_2 and 20KNN-80TeO_2 samples heat treated at their T_{c2} are opaque. The effect of HT temperature on the transparency of glass originates from the type and size of crystals precipitated in the glass matrix. For visible light, samples possessing crystals larger than 200 nm should show light scattering and hence the respective samples should be opaque. The transparent samples should contain crystals << 200 nm and also a small crystal size distribution. For 30KNN-70TeO_2 glass-ceramics, the crystal size may play an important role in the transparency of the glass-ceramics as the increase in HT temperature caused the decrease in transparency up to the HT 350 ^oC. This is consistent with the XRD result where the crystallinity of the (K,Na)NbO_3 crystals increased with increasing HT temperature. When the HT temperature was 420 ^oC, a secondary phase of $KNbTeO_6$ occurred and reduced the transparency of the glass ceramic greatly. For the 20KNN-80TeO_2 glass-ceramics, there is no good tendency between transparency and HT temperature.

Considering their corresponding XRD patterns, only one crystal phase of cubic (K,Na)NbO_3 was observed in all glass-ceramics with HT temperature from 300 ^oC – 408 ^oC. The highest degree of crystallinity was found in the glass-ceramic sample with HT of 408 ^oC, while other lower HT temperature samples (300-350 ^oC) possess similar crystallinity. It may be assumed that the crystal sizes in these 20KNN-80TeO_2 glass ceramic series may come from the inhomogeneous

distribution of the cubic $(K,Na)NbO_3$ in the glass matrices. The corresponding SEM micrographs of these glass-ceramics are shown in Fig. 4.8 and 4.9.

2) Refractive index and energy band gap

In Fig. 4.16 shows the refractive indices of the heat treated glass-ceramics at various temperatures. It can be noted that the overall refractive indices of $30KNN\text{-}70TeO_2$ glass-ceramics are lower than that of $20KNN\text{-}80TeO_2$. This consistent with the density result, as in general the higher density of glass is, the greater refractive index is obtained.

Energy band gap from the transmission cut-off wavelength (Eg) was shown in Fig. 4.17 and summarized in Table 4.3. The refractive index of all glasses are lying between 2.00 – 2.20. The optical band gap was obtained by plotting $(\alpha hv)^2$ versus hv (where α is the absorption coefficient and hv is the photon energy), which is described by equation 4.3 [113-114].

$$\alpha hv=(hv-Eg)^{1/2} \quad (4.3)$$

Where α is the absorption coefficient, h is Planck's constant, v is the photon frequency, and E_g is the band gap energy. The absorption coefficient α is obtained from Beer's law equation 4.4.

$$\alpha=-(lnT)/t \quad (4.4)$$

Where t is the thickness of the measured sample and T is transmittance. The optical band gap, E_g of selected glass and glass-ceramics, varied between 2.35 and 2.90 eV.

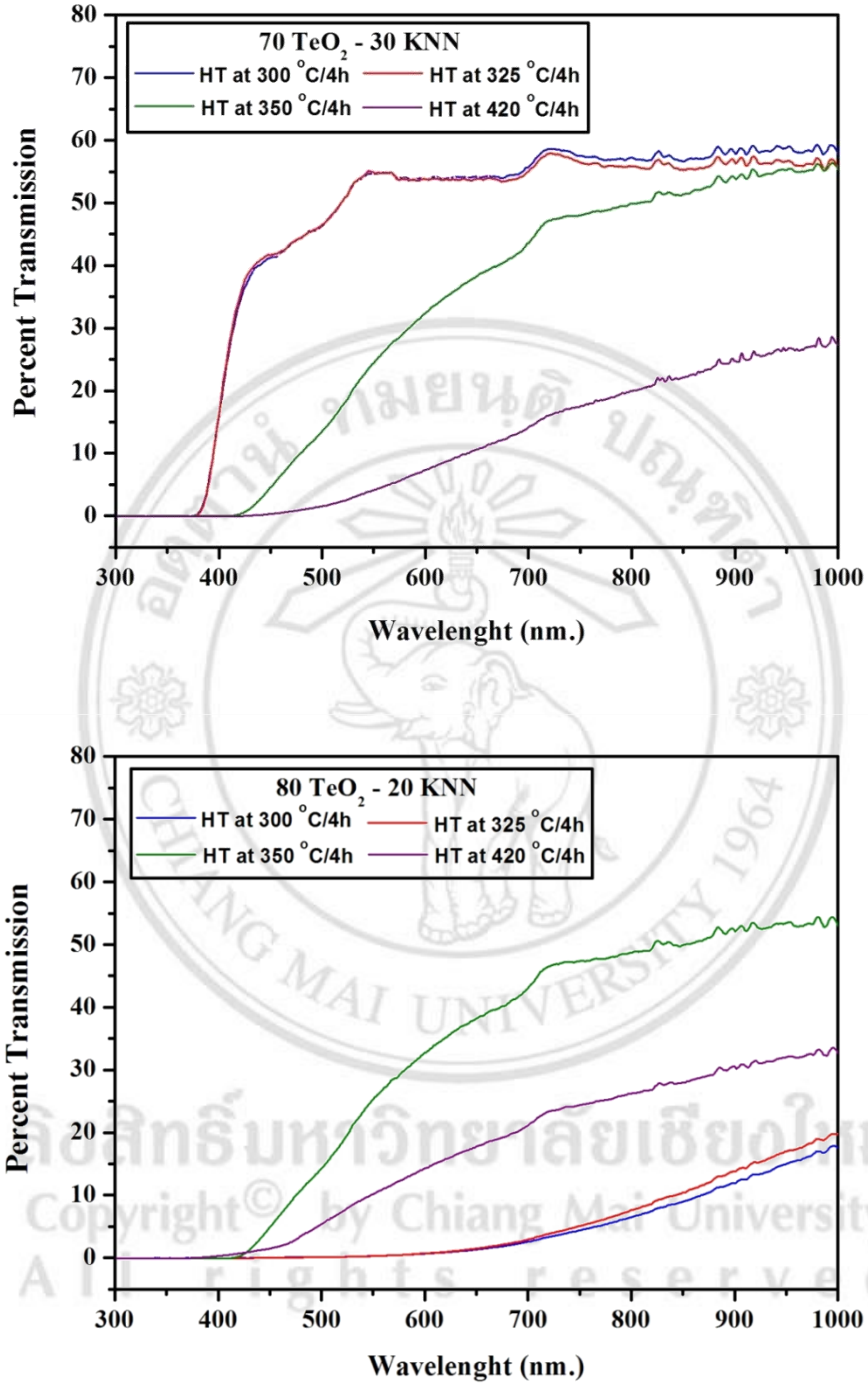

Figure 4.15 The percent transparent of glass-ceramic which heat treated at various temperatures.

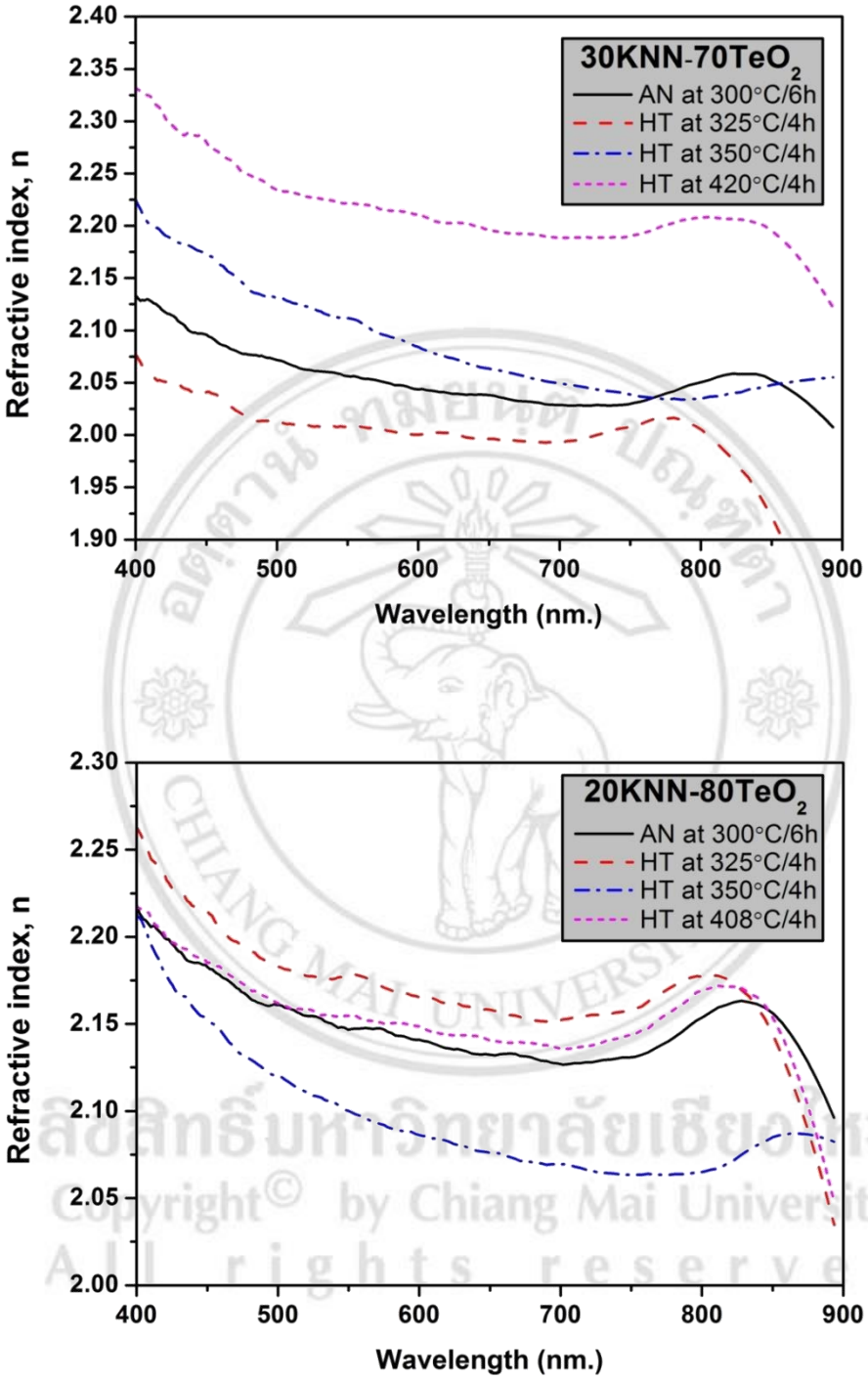

Figure 4.16 Refractive index of glass-ceramic which heat treated at various temperatures.

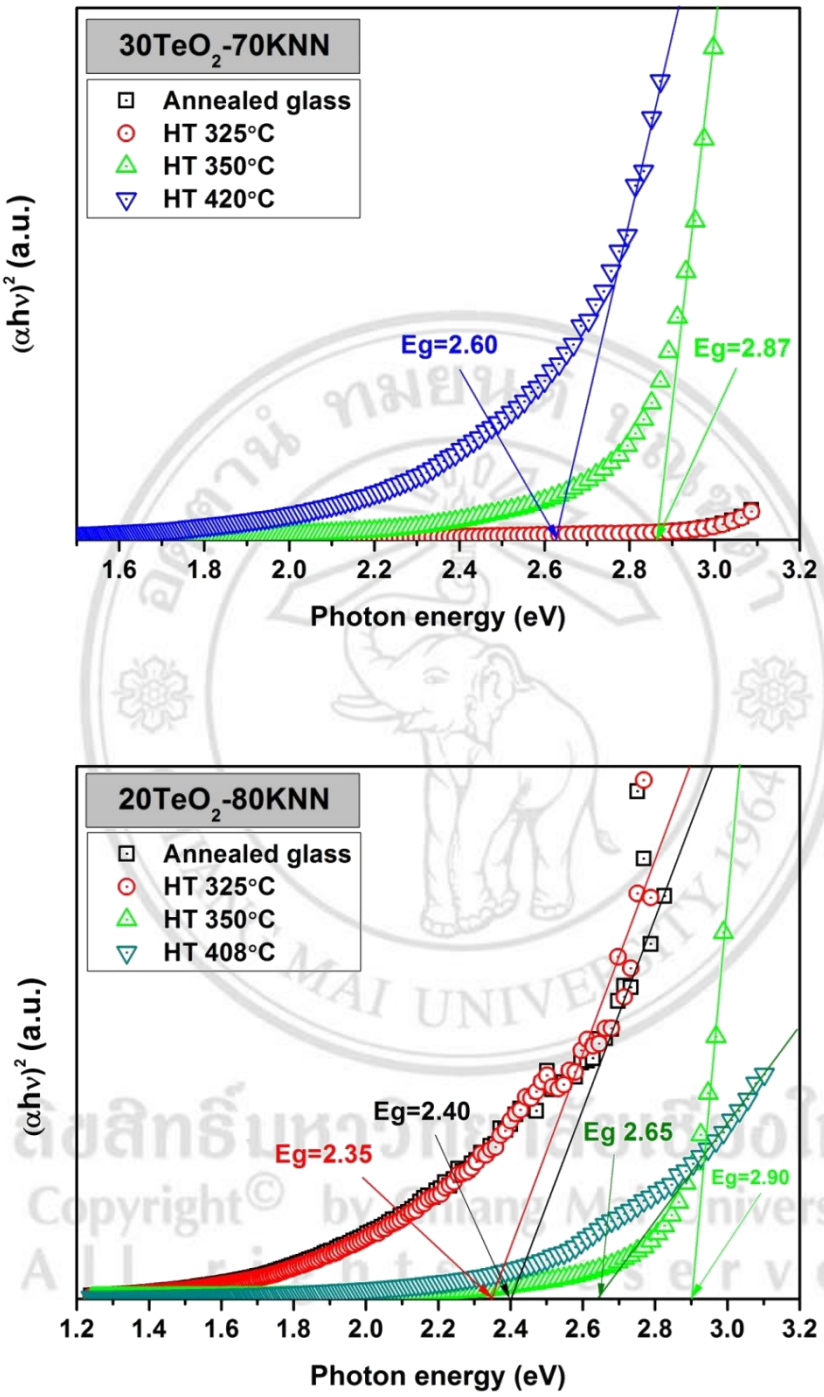

Figure 4.17 Photo energy of glass-ceramics 30KNN-70TeO_2 and 20KNN-80TeO_2.

Table 4.3 Refractive indices of various heat treatment temperature glass-ceramics samples of two glass composition.

Heat treatment temperature (°C)	Refractive index of HT glasses (at 532 nm.)	Energy band gap (Eg; eV)
30KNN- 70TeO_2		
300	2.090	-
325	2.012	-
350	2.086	2.87
420 (T_{c1})	2.154	2.60
20KNN- 80TeO_2		
300	2.165	2.40
325	2.183	2.35
350	2.089	2.90
408 (T_{c1})	2.177	2.65

4.1.7 Conclusions

Various materials characterization techniques were performed to study the effect of heat treatment temperature on physical, phase, dielectric and optical properties of KNN-TeO_2 glass-ceramics prepared via incorporation method. It was found that the amount of KNN in glass controlled the thermal stability of glass where a higher amount of KNN (30 mol%) promotes the stability of the glass. The XRD revealed similar crystals phase of cubic (K,Na)NbO_3 in all glass-ceramics with low HT temperature of 300°C–350°C. The glass-ceramics heat treated at T_{c1} and T_{c2} of each glass composition contained additional $Na_2Nb_4O_{11}$, $KNbTeO_6$ and TeO_2 with amount depending on the added KNN content. The crystal phases and their sizes in turn play the most important role in controlling physical, appearance, density, dielectric and optical properties of the heat treated glass-ceramics. It was found that the larger amount of KNN (30 mol%) gave improved properties of the glass-ceramic, as a glass-ceramic with high transparency, good mechanical and high dielectric constant could be obtained. Further studies should add for more understand KNN-TeO_2 phenomena.

4.2 The characterization of Er_2O_3 doped KNN-TeO_2 glass and glass-ceramic

In this section, the effect of doped Er_2O_3 in KNN-TeO_2 glass has been carried out. Er_2O_3 is a rare-earth element that was very useful in many applications such as light emitting diode display, laser diode and etc., because of their electrical, optical and photoluminescence properties. The interesting characteristic of this material is the energy transfer of electrons by convert to higher or lower energy which is very good in promoting photoluminescence media. In this work, 30KNN-70TeO_2 was chosen to be base glass because of their good stability and optical property as mentioned previously in section 4.1. The well prepared KNN single phase ceramic powders from incorporation method were mixed with TeO_2, and then Er_2O_3 was doped in range of 0.5-1.0 mol%. Moreover, melting temperature and dwelling time were set in different range depends on their thermal analysis for studied the effect of temperature in melting-quenching and heat treatment process, to find the proper condition in prepared glass-ceramics 30KNN-70TeO_2.

4.2.1. Thermal behavior determination

From section 4.1, it can be found that glass-ceramics in composition of 30KNN-70TeO_2 are steady rather than 20KNN-80TeO_2. This optimized condition was selected to dope with Er_2O_3 of about 0.5-1.0 mol%. The weight percent of 30KNN-70TeO_2 doped with Er_2O_3 glasses are already calculated and showed in table 3.3, in chapter 3. Here, melting temperatures were varied between 800-900°C for 15 minutes to 1 hour. At first, 0.5 mol% of Er_2O_3 doped in 30KNN-70TeO_2 glass was studied for estimated the optimize composition of glass by melting at 800°C for 15min - 30min. Then, 1.0 mol% of Er_2O_3 doped in 30KNN-70TeO_2 glass was studied by melting at 800°C - 900°C for 30min - 60min. The increased of dwell time in glass composition of 1.0 mol% Er_2O_3 dopant were presumed to raise the stability of glasses, because the low strength and difficult to handle of 0.5 mol% of Er_2O_3 dopant glass sample. The appearances of as-received glasses were orange in color, high transparent and quite low mechanical strength. All of glass compositions were symbolized as the capital letter and showed in Table 4.4.

In Table 4.4 also show the attempt study in tendency of glass stability which were done by using DTA data analysis, and put the DTA profile of 30KNN-70TeO_2 glass without dopant which melted at 800°C for 15min – 30min for comparing to glass with dopant. Densities of as-received glasses were showed in Table 4.4. The densities of all glasses are high when comparing with another glass types such as silicate glass and borate glass etc. The melting and annealing temperature are plays a significant role in controlling density. Thus, it might be one of the variable controls of the crystallization in glass.

The DTA analyses were recorded for the precursor glass powder and are shown in Fig. 4.18. In glass composition of 30KNN-70TeO_2 which melted for 15min (series A.) and 30min (series B.) were shown glass transition or T_g around 325°C. After added 0.5 mol% of Er_2O_3, the T_g point was shifted to 350°C (series C. and D.). Then, in glass system of 1.0 mol% of Er_2O_3 was exhibited higher T_g point in 4.the temperature ranging between 375°C to 388°C. All glass conditions (A.-H.) showed 2 exothermic peaks, names T_{c1} and T_{c2} which were defined as crystallization temperature. Those transition and crystallization temperature were increased with increasing Er_2O_3 contents and those increasing trend were also found in the increased of heat treatment temperature and times (systems E.-H.). The individual peak at 580°C is the standard reference peak of SiO_2. This obviously peak was not found in the first 2 systems (A.-B.) because of the reference standard is Al_2O_3.

From the DTA data, the glass thermal stability factor (equation 4.2) has been determined and showed in Table 4.4. It was found that glass without Er_2O_3 showed highest stability factor. While Er_2O_3 concentration was increased, the stability factor of glass has decreased. This may result from the large molecular mass of Er_2O_3 which is accommodated in the open structure of the TeO_2 glassy state. This may reduce the ability of a compact glass structure and lead to the lower stability of the Er_2O_3 doped-glasses [107]. In Er_2O_3 doped glasses, the most stable glass was found in glass C. and D. using the melting temperature and dwell time of 800°C and 15min - 30min, respectively, with the stability factor of approximately 67°C and 68°C. The high thermal stability factor identifies the ability of glass to form nano-

structured glass–ceramics which can be control by heat treatment process.

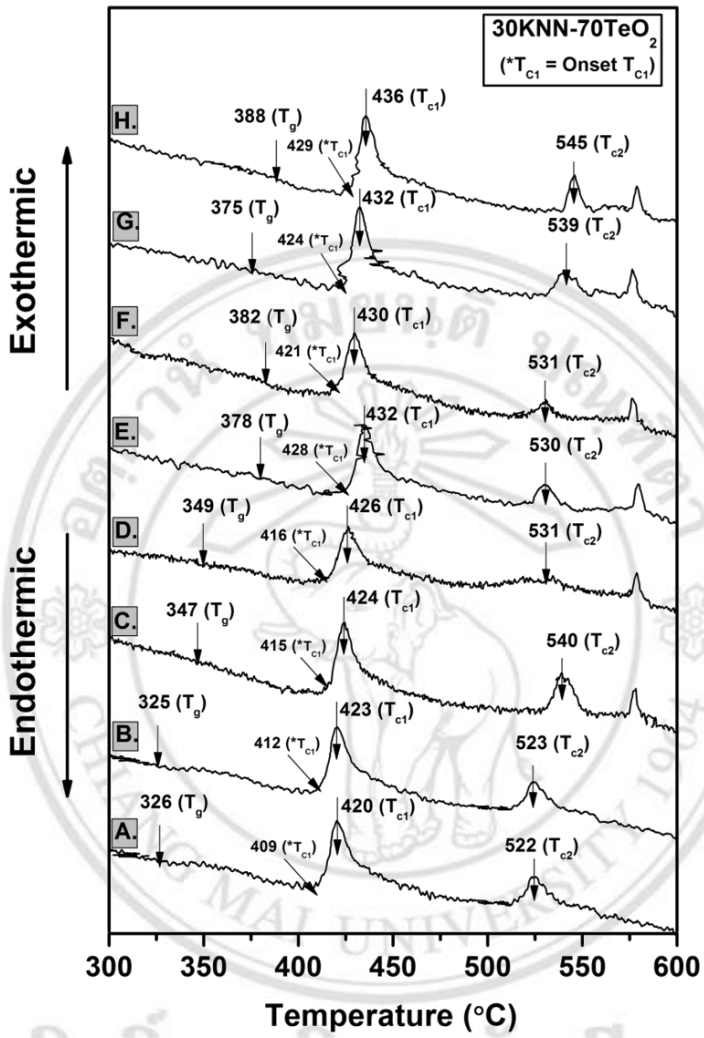

Figure 4.18 Thermal analysis of 30KNN-70TeO2 glass doped with 0-1 mol% of Er2O3. **(A.-B.)** Glass composition of 30KNN-70TeO_2. **(C.-D.)** Glass composition of 0.5 mol% Er_2O_3 doped 30KNN-70TeO_2. **(E.-H.)** Glass composition of 1.0 mol% Er_2O_3 doped 30KNN-70TeO_2.

Table 4.4 Density and thermal profile data of all glass samples.

Melting temperature (°C/min)	Density (g/cm^3) Quenched	Density (g/cm^3) Annealed	DTA				
			T_g	$*T_{c1}$	T_{c1}	T_{c2}	ΔT
30KNN-70TeO_2							
(A.) 800°C/ 15 min	4.75	4.78	326	409	420	522	83
(B.) 800°C/ 30 min	4.77	4.78	325	412	423	523	87
30KNN-70TeO_2 doped 0.5 Er_2O_3							
(C.) 800°C/ 15 min	4.64	4.70	347	415	424	540	**68**
(D.) 800°C/ 30 min	4.82	4.85	349	416	426	531	**67**
30KNN-70TeO_2 doped 1.0 Er_2O_3							
(E.) 800°C/ 30 min	4.82	4.84	378	428	432	530	50
(F.) 800°C/ 60 min	4.87	5.06	382	421	430	531	39
(G.) 900°C/ 30 min	4.80	4.81	375	424	432	539	49
(H.) 900°C/ 60 min	4.75	5.05	388	429	436	545	41

*T_{c1} = The onset point of T_{c1}

Then, we chose the optimum condition of 30KNN-70TeO_2 doped with 0.5 - 1.0 mol% Er_2O_3 for subjecting to the heat treatment schedules depending on their thermal profiles to form glass-ceramics. The selected glasses were then heat treated at different temperature at above T_g point to T_{c2} for 4 hours with heating rate of 5°C/min to study the evolution of phase formation in glass-ceramics. Samples of glasses and glass-ceramics are displayed in Fig. 4.19 – 4.20. The transparency was found to decrease with increasing heat treatment temperature.

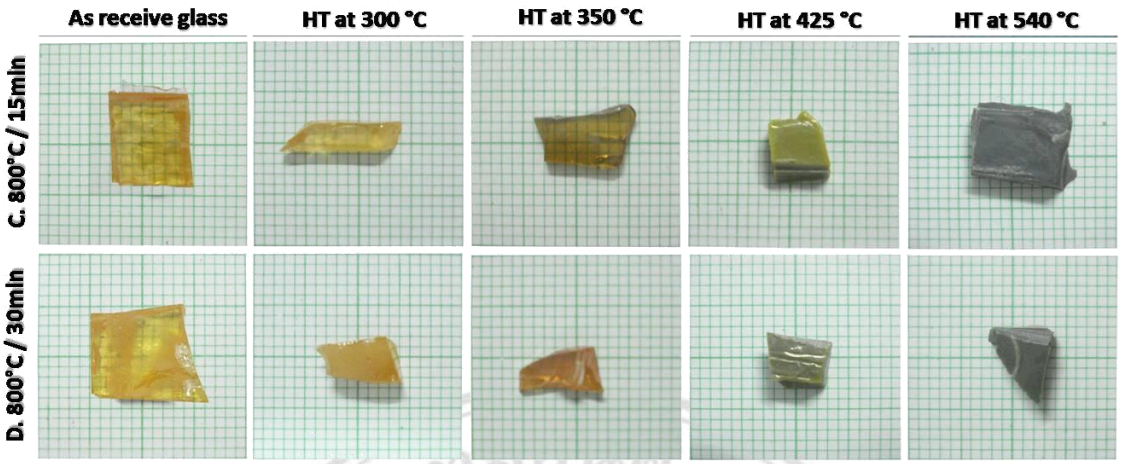

Figure 4.19 The appearances of glass 30KNN-70TeO2 doped with Er_2O_3 of about 0.5 mol% and heat treatment for 4 hours at various temperatures.

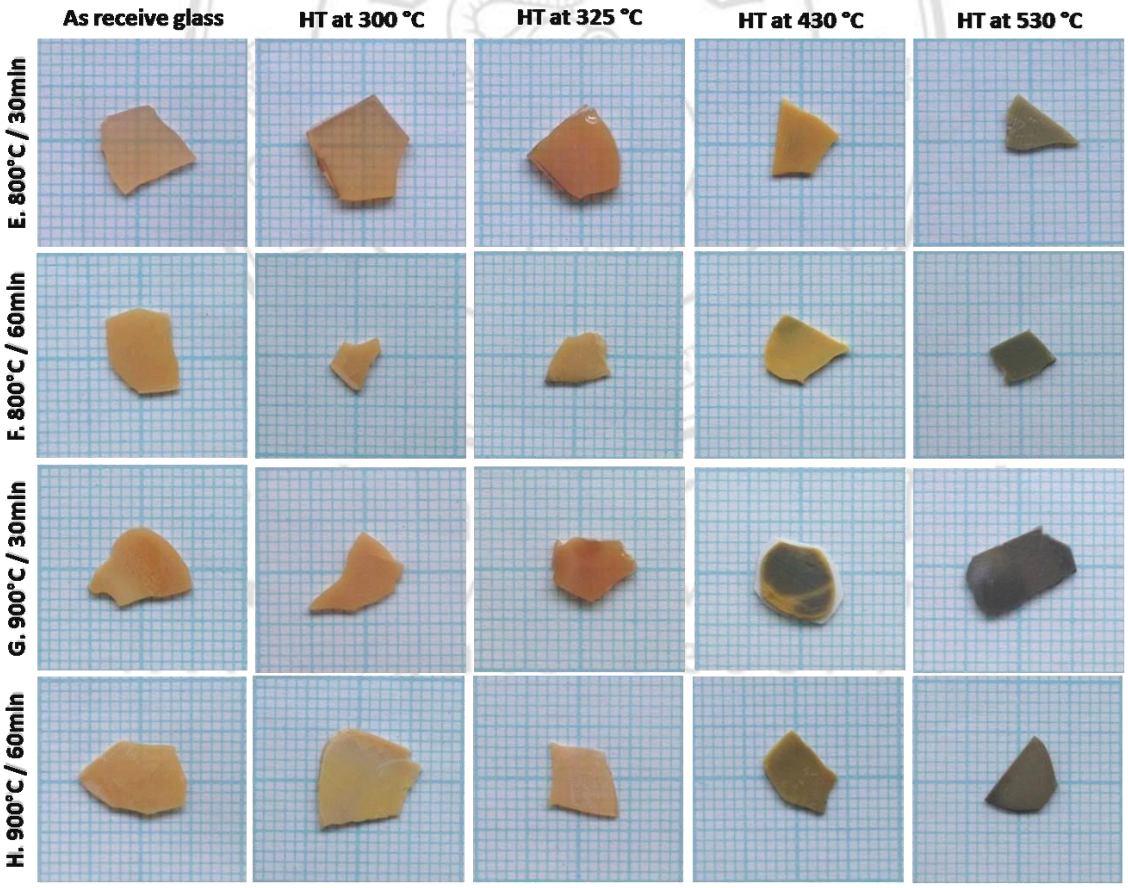

Figure 4.20 The appearances of glass 30KNN-70TeO_2 doped with Er_2O_3 of about 1.0 mol% and heat treatment for 4 hours at various temperatures.

4.2.2. Densification investigation

The densities of glass-ceramics doped with Er_2O_3 showed similar trend. The density of heat treated glass increased with increasing heat treatment temperature as shown in Fig. 4.21 and 4.22. This corresponds to the volume of crystallization during the heat treatment process. At room temperature, it can be seen that their densities are lowest because of no crystalline phase in glass matrix are exit. This result can be confirmed by XRD analysis. Glass-ceramics samples of highest heat treatment temperature have higher density than that of the sample heat-treated at lower temperatures, showing that the heat treatment process is essential parameter in controlling the crystallization of the glass-ceramics. The heat treatment time is also one of the important parameters in particular. The time spending in this process, can raise the density of glass by increasing dwell time.

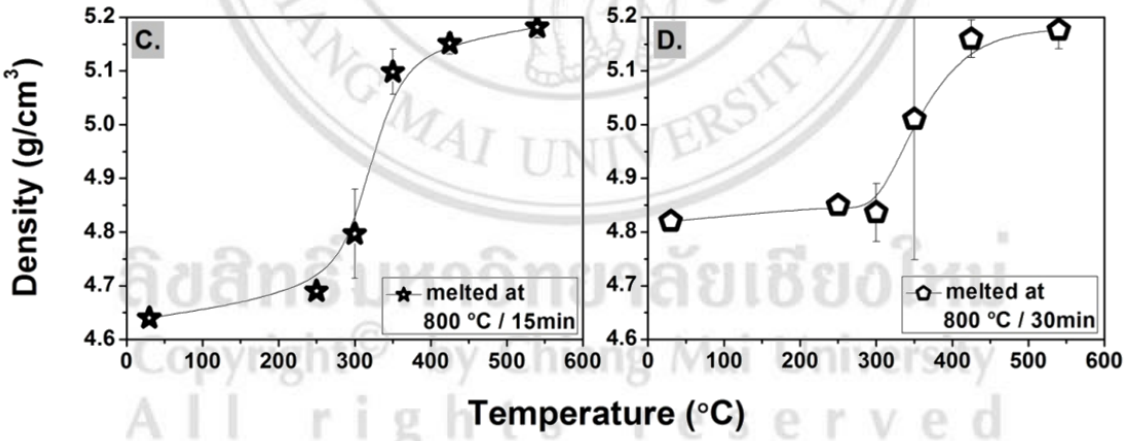

Figure 4.21 Density of glass ceramics 30KNN-70TeO_2 doped with 0.5 mol% Er_2O_3 in system C. and D.

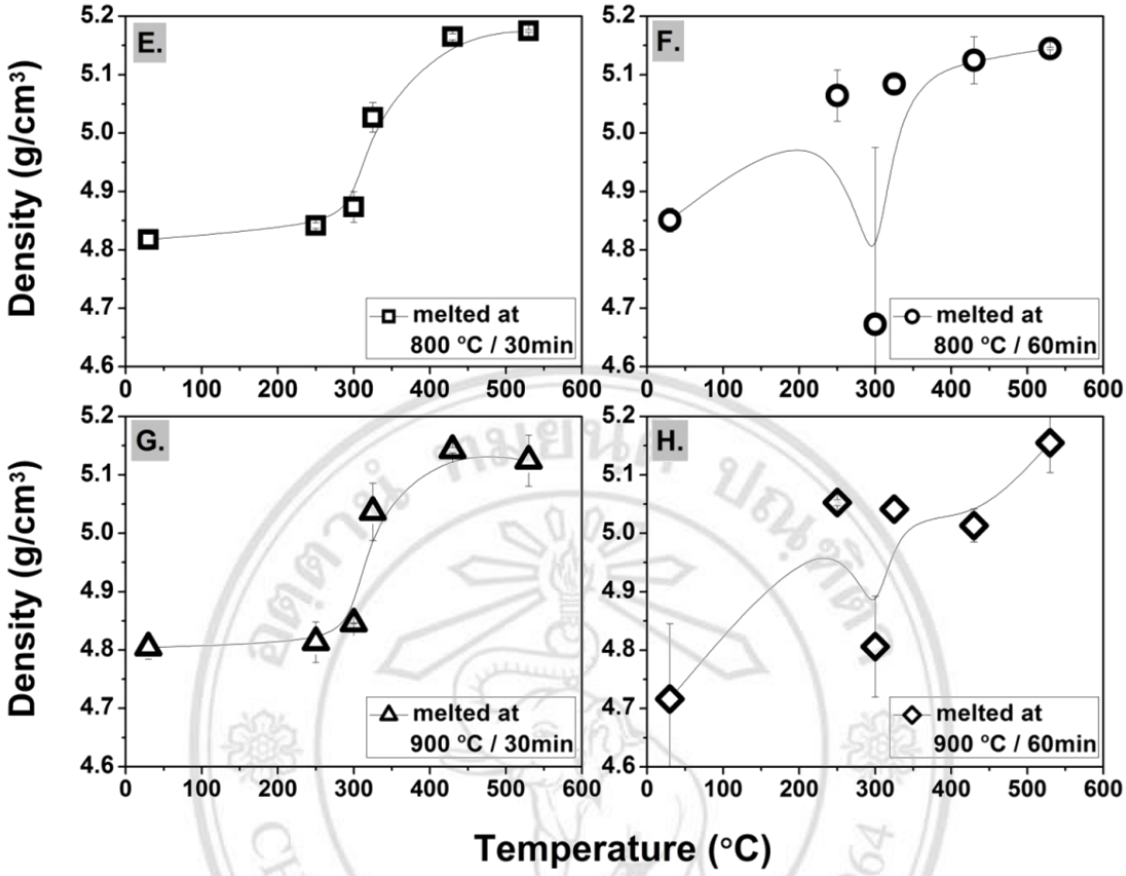

Figure 4.22 Density of glass ceramics 30KNN-70TeO_2 doped with 1.0 mol% Er_2O_3 in system E., F., G., and H.

4.2.3. Structural formation

In Fig. 4.23-4.25, the XRD results of the heat treated glass-ceramics contains no tetragonal or monoclinic KNN; $(K_{0.5}Na_{0.5})NbO_3$ crystal phase. This may be due to two reasons, first, the very low viscosity of telluride glasses at their melting temperatures; 800°C and 900°C, giving rise to compositional fluctuation, another one is, because the melting temperature of TeO_2 is relatively low (732°C), therefore it is easily evaporated resulted in the slightly change in glass compositions during metling at elevated temperature [115]. At a heat treatment temperature below 300°C (annealing temperature), the resulting glass-ceramics showed nearly amorphous patterns with a very small trace of crystalline peaks of cubic $(K,Na)NbO_3$ phase. When heat-treated at 325°C-350^{o}C, glass-ceramics exhibited obvious crystalline peaks, which may

be identified as the typical cubic (K,Na)NbO_3 phase with random variation of K and Na ions in the A-site of the unit cell [116].

The heat treated samples at T_{c1} and T_{c2} for each glass composition are also illustrated. Glass ceramics heat treated at T_{c1} contained two other phases apart from the cubic (K,Na)NbO_3 phase (*), which may be identified as $KNbTeO_6$ (●) and $Na_2Nb_4O_{11}$ (♦). At T_{c2}, the additional α-TeO_2 (⊙) phase was clearly revealed in all glass ceramics, together with two phases of $KNbTeO_6$ (●) and $Na_2Nb_4O_{11}$ (♦).

It may be assumed that the intensity of glass melted for 60min was not different from glass melted for 30min, meaning that the melting time has slightly affected on the crystallization in glass-ceramics. This may be due to the slightly different in stability factors of these glasses which lie between 48°C - 57 °C. It can be also seen that the glass-ceramics heat treated around T_{c1} and T_{c2} have differences in degree of crystallinity.

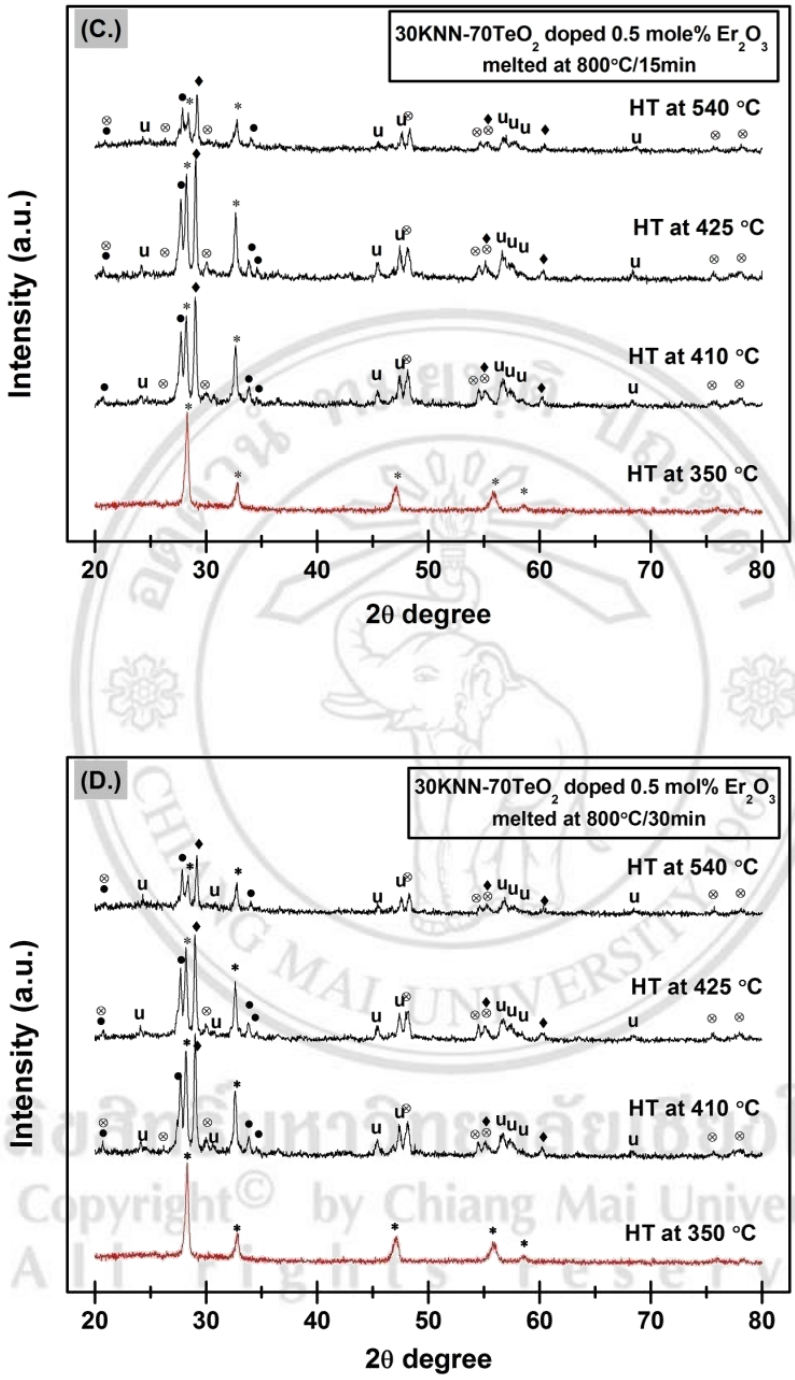

Figure 4.23 XRD pattern of glass ceramics 30KNN-70TeO_2 doped with 0.5 mol% Er_2O_3 in system C. and D. (melted at 800°C for 15min (C.) and 30min (D.), respectively) after heat treatment at various temperature.

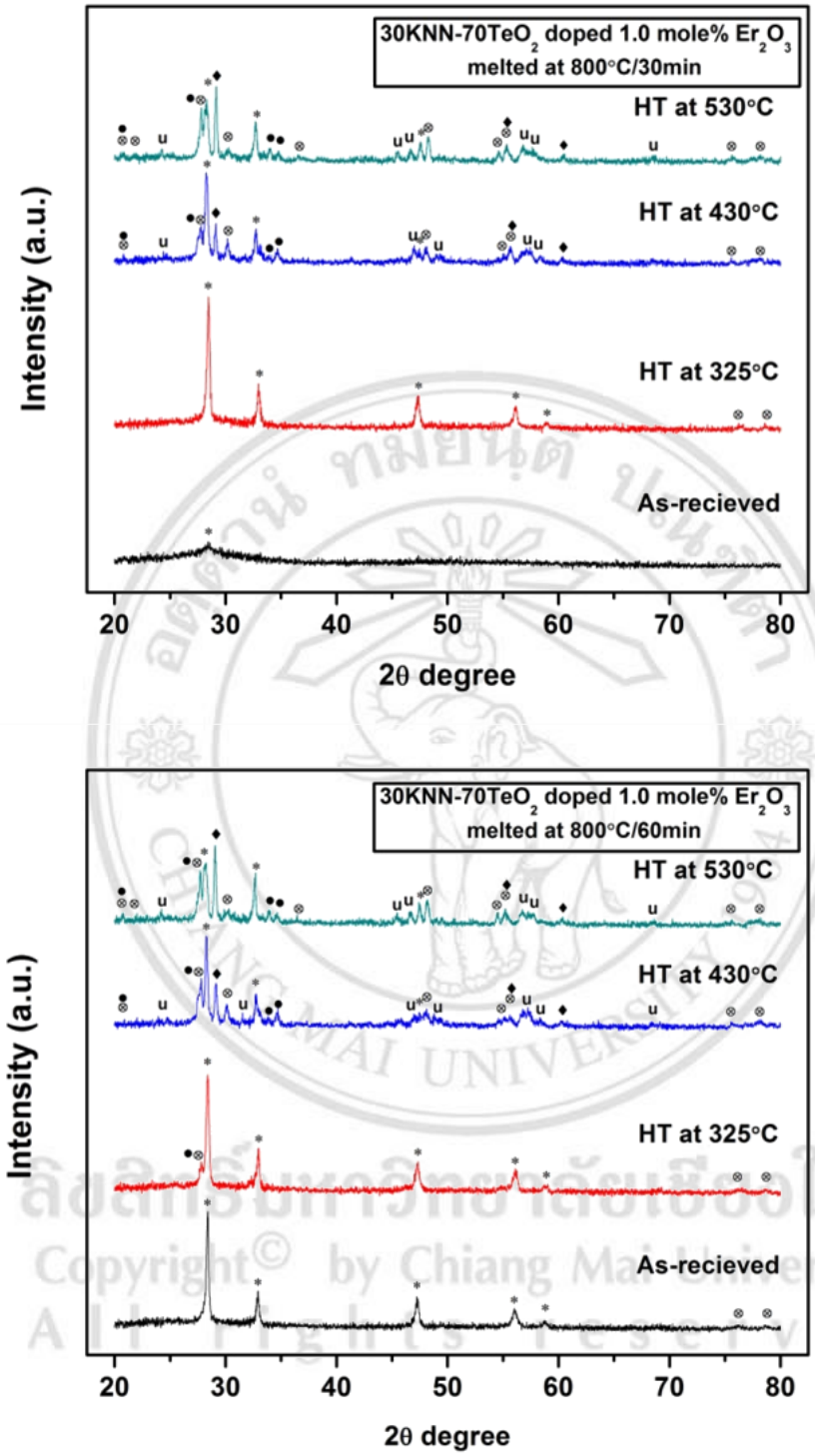

Figure 4.24 XRD patterns of glass ceramics 30KNN-70TeO_2 doped with 1.0 mol% Er_2O_3 in system E. and F. (melted at 800°C for 30min (E.) and 60min (F.)) after heat treatment at various temperature.

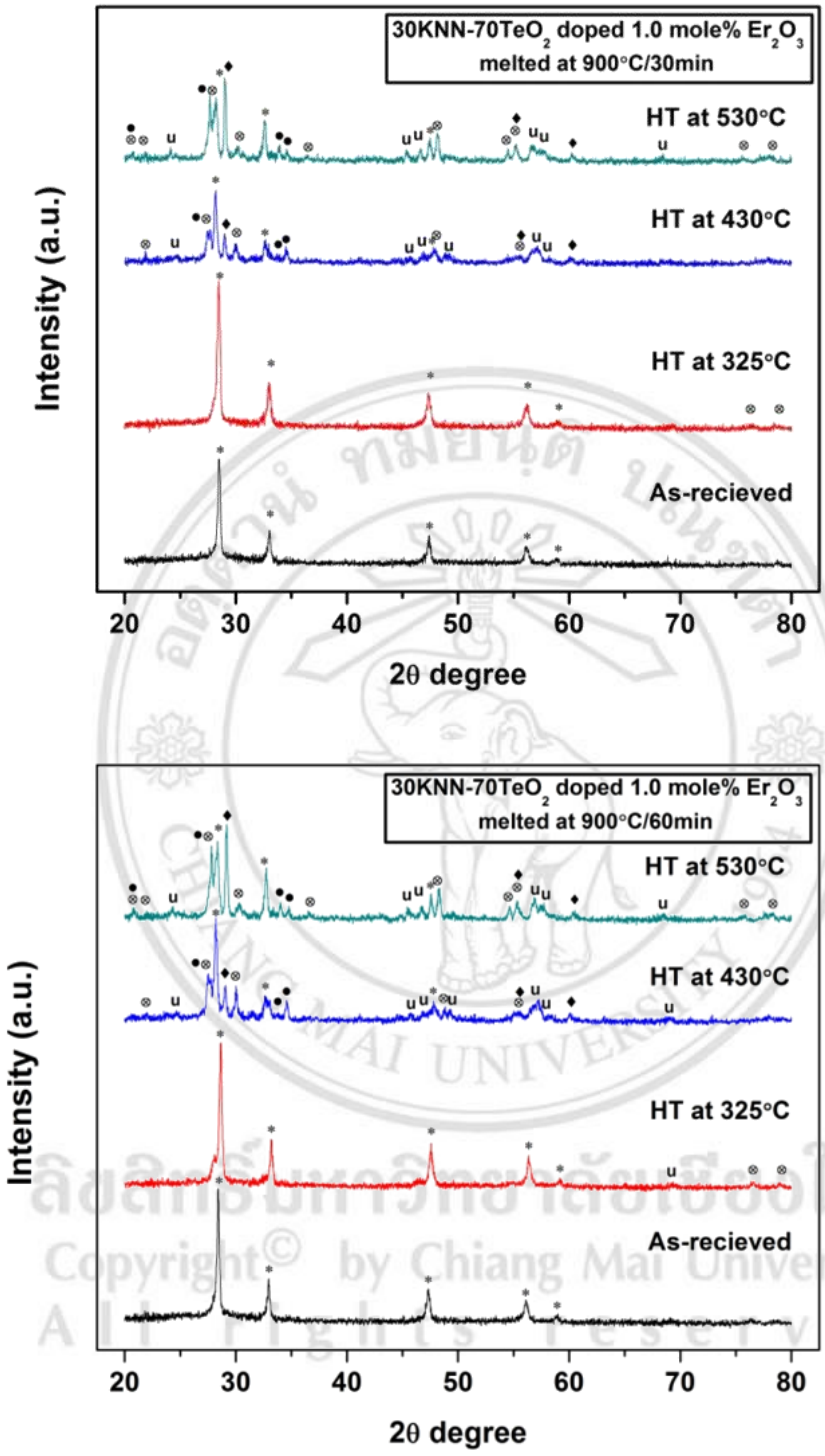

Figure 4.25 XRD patterns of glass ceramics 30KNN-70TeO_2 doped with 1.0 mol% Er_2O_3 in system G. and H. (melted at 900°C for 30min (G.) and 60min (H.)) after heat treatment at various temperature.

4.2.4. Microstructure observation

FE-SEM micrographs of cross-sectional morphology of Er_2O_3 doped 30KNN-70TeO_2 glasses and glass-ceramics heat-treated at various temperatures and T_{c1} and T_{c2} for 4 hours were illustrated in Fig. 4.26 and 4.27, respectively. SEM micrographs of the glass ceramics with 0.5 mol% of Er_2O_3 are shown in Fig. 4.26. These micrographs show a bulk crystallization of the KNN phase with a different shapes observed for the glass matrices of all heat-treated samples. At 425°C, the rod crystal shape was observed and gradually changed to rectangular shape around 540°C. Then at 560°C, crystals changed to cubic shape. The average crystal sizes observed from the SEM micro-graphs are summarized in Table 4.5. It can be seen that all of the glass-ceramics have crystal size lower than 1 μm. but still too large (>200 nm.) to be transparent, giving rise to opaque bulk glass-ceramics. This is consistent with the XRD result. The crystallinity of the solid solution of (K,Na)NbO_3 crystals increased with increasing HT temperature. The highest degree of crystallinity (with diagonal value of 664±468 nm.) was found in the glass-ceramic sample melted at 800◦C for 15min and HT at 540°C.

In Fig. 4.27, after heat treated glass with 1.0 mol% of Er_2O_3 at lowest heat treatment temperature of 325°C, no crystalline evidence is clearly revealed by using secondary electron image (SEI) mode. This may be caused by the different in crystallite size of the cubic (K,Na)NbO_3 phase in this glass-ceramics, however, the careful study such as sherrer equation should be performed to confirm this assumption. The small bulk crystallization of the KNN crystals with rectangular shape occured at 430ºC. After higher heat treatment temperature, irregular shape of crystals is revealed. The crystals of all samples are homogeneously embedded throughout the glass matrix with random orientations. However, by using SEI mode the atomic contrast between the cubic KNN phase and other co-precipitated phases could not be revealed.

(C.)

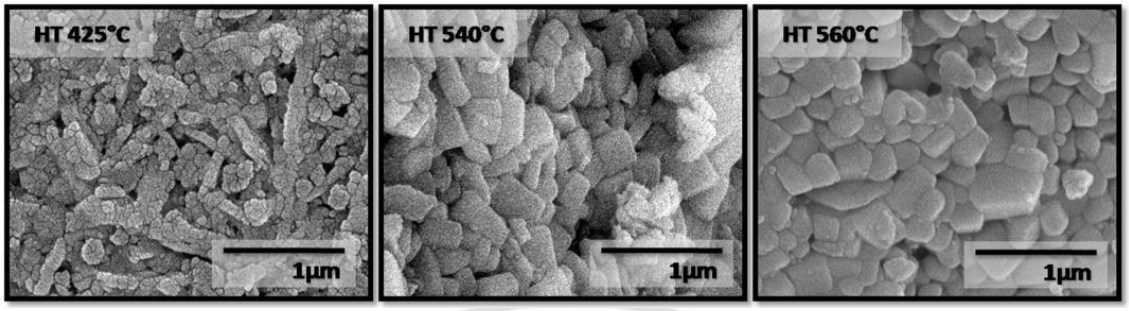

(D.)

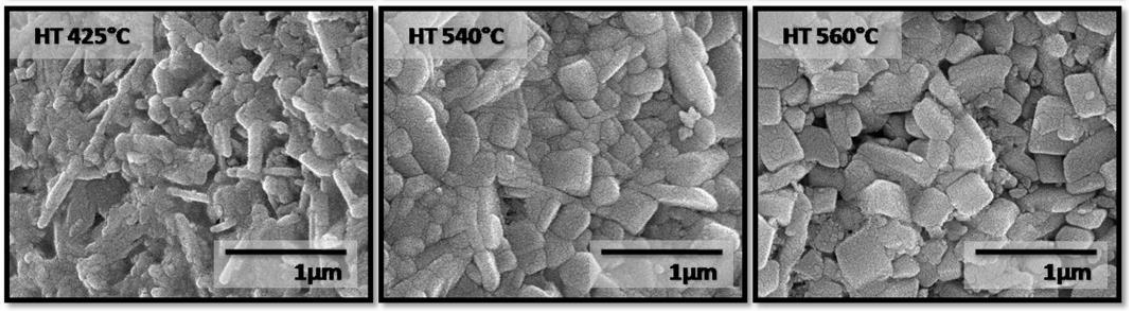

Figure 4.26 SEM micrographs of glass ceramics 30KNN-70TeO_2 doped with 0.5 mol% Er_2O_3 in system C. and D. (melted at 800°C for 15min (C.) and 30min (D.), respectively) after heat treatment at various temperature.

Table 4.5 Summary of crystal morphology and crystallite sizes.

Condition (mol%) 70KNN-30TeO_2 doped 0.5 Er_2O_3	**Heat treatment temperature (°C)**	**Average crystal size (nm.)**	
		L[a.]	**D**[b.]
800°C/ 15 min	425	147±17	-
	540	406±95	664±468
	560	474±43	157±17
800°C/ 30 min	425	107±7	-
	540	791±75	375±33
	560	-	433±22

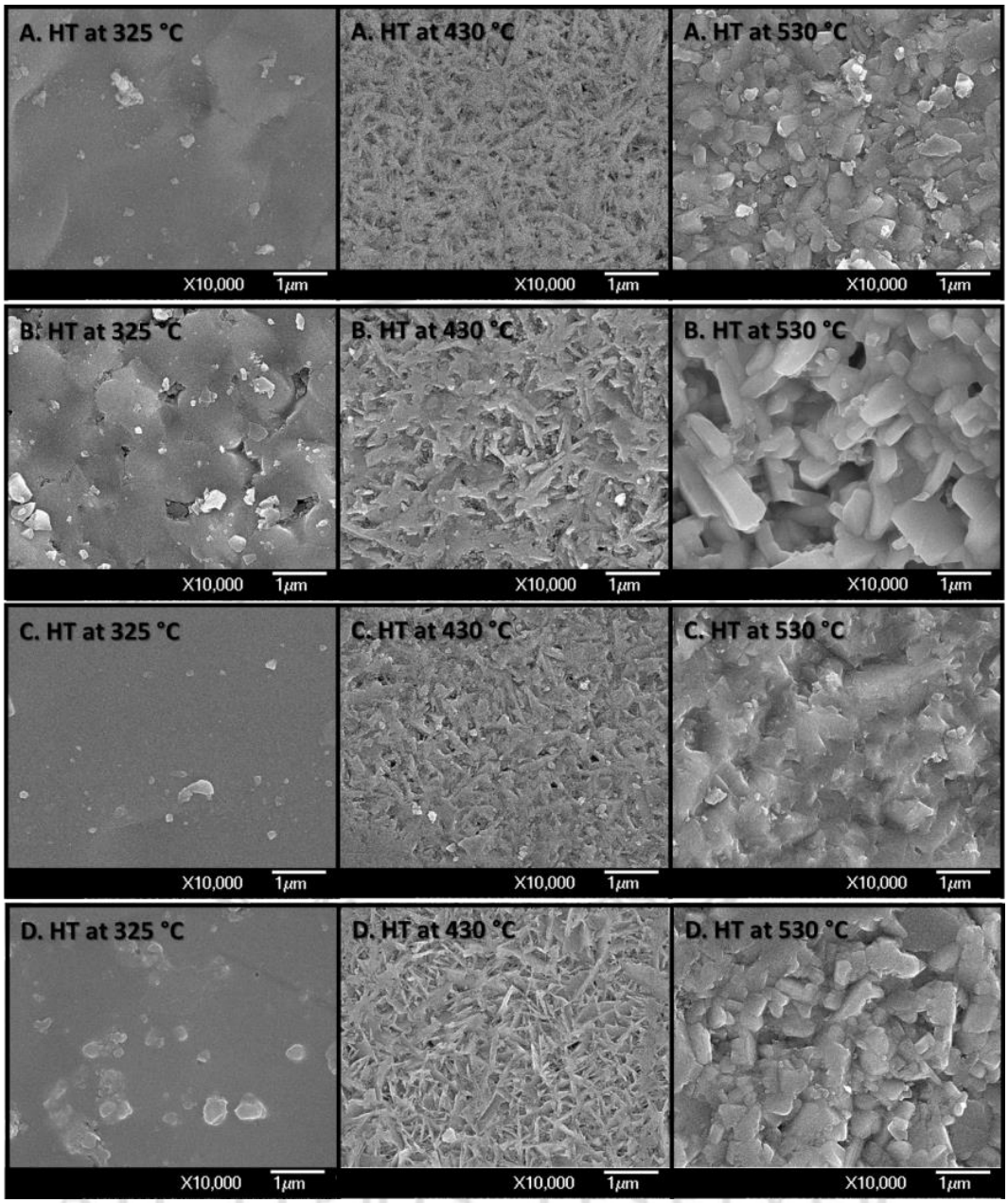

Figure 4.27 SEM micrographs of glass ceramics 30KNN-70TeO_2 doped with 1.0 mol% Er_2O_3 in system E., F., G. and H. (melted at 800°C for 30min (E.) and 60min (F.) and melted at 900°C for 30min (G.) and 60min (H.)) after heat treatment at various temperature.

4.2.5. Electrical property

Dielectric constants of the glass-ceramics from the two glass series (C.) melted at 800°C for 15min and (D.) melted at 800°C for 30min at various heat treatment temperatures are shown in Fig. 4.28. The maximum dielectric constant of about 625 at 100 kHz was found in the glass-ceramics from the glass C. It can be also observed that overall values of dielectric constant of the glass-ceramics form the glass series C. are higher than those of the glass series D. It may then be assumed that the longer dwell time of 30min had significant effect on dielectric properties. This long dwell time caused more compositional fluctuation of glass series D. From the dielectric result, it was found that, the lower heat treatment temperatures of 300 and 350°C offered the transparent glass-ceramics from the series D. glass with high dielectric constant.

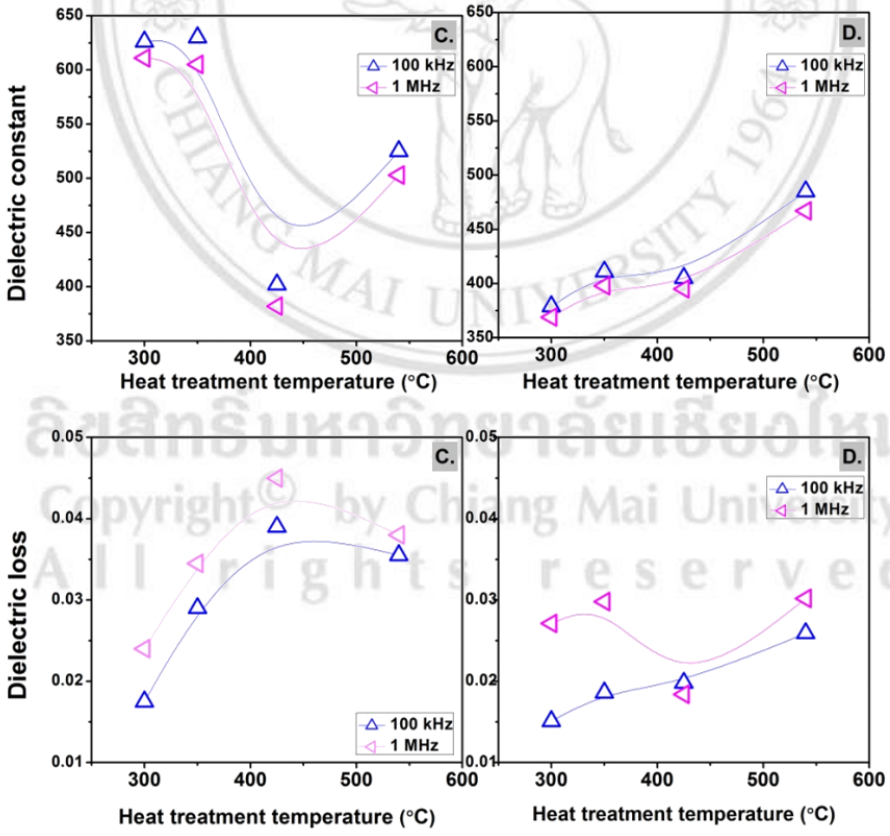

Figure 4.28 Dielectric constants and dielectric losses of glass ceramics 30KNN-70TeO_2 doped with 0.5 mol% Er_2O_3 in system C. and D. (melted at 800°C for 15min (C.) and 30min (D.), respectively) after heat treatment at various temperature.

In Fig. 4.28, shows the dielectric properties of the heat treated glass-ceramics at various temperatures. The maximum dielectric constant was found in glass ceramic G. heat treated at T_{c2}, which was as high as 800 at 1 kHz and the dielectric loss was rather low about 0.01. It can be seen that the dielectric constant decreased when increasing frequency. This may be due to the fluctuation of glass composition which is evidenced by the different in stability factor of each glass condition.

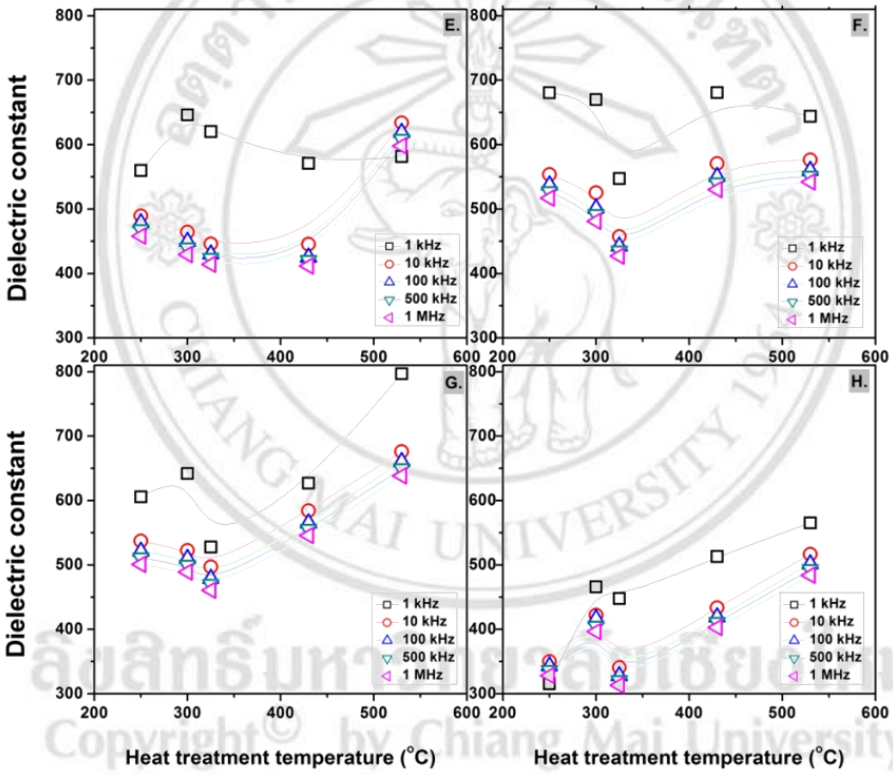

Figure 4.29 Dielectric constants of glass ceramics 30KNN-70TeO_2 doped with 1.0 mol% Er_2O_3 in system E., F., G. and H.

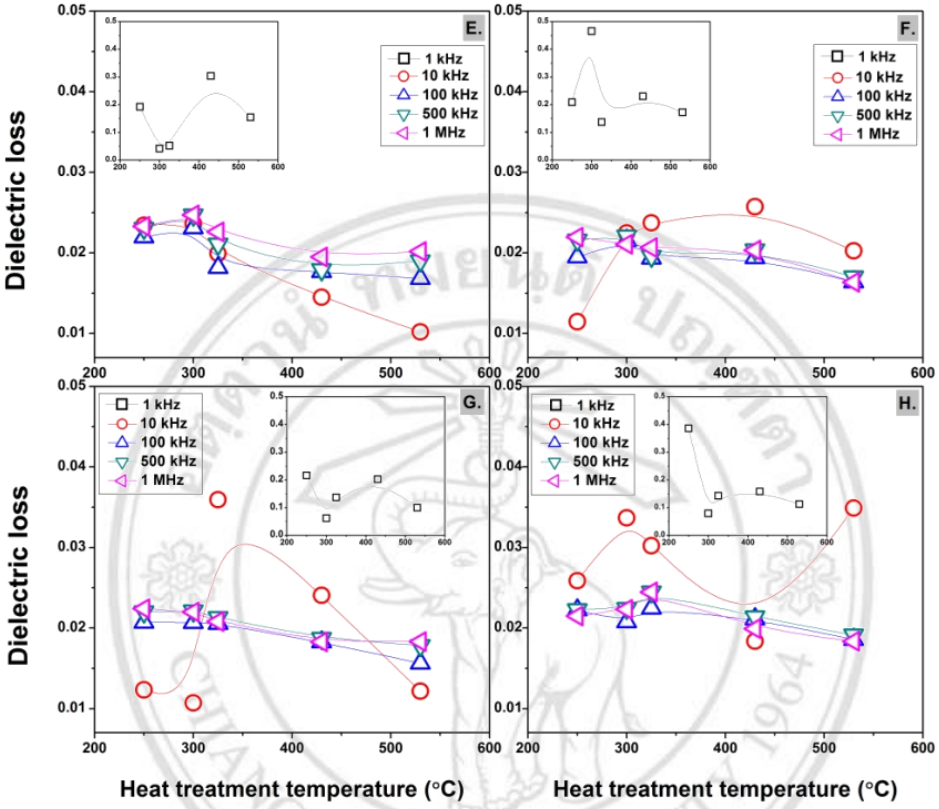

Figure 4.30 Dielectric losses of glass ceramics 30KNN-70TeO_2 doped with 1.0 mol% Er_2O_3 in system E., F., G. and H.

4.2.6. Optical properties

1) Absorbance

Glass and glass-ceramics UV-Vis absorption (Abs) is shown in Fig. 4.31. It can be seen that the minimum absorption was found in as-received glass and then the absorption decreased with increasing heat treatment temperatures until light cannot get through glass-ceramics heat-treated at higher temperature (T_{c1} and T_{c2}). The effect of HT temperature on the transparency of glass originates from the type and size of crystals precipitated in the glass matrix. For visible light, samples containing crystals larger than 200 nm cause light scattering and hence the respective samples should be opaque. Transparent samples should contain crystals lower than 200 nm and also a small crystal size distribution.

From Fig. 4.31, the absorption of 0.5 mol% Er_2O_3 doped glass and glass-ceramics display strong absorption edges below 350 nm and show the distinct erbium absorption peaks which are similar to previous work in silicate and tellurite glasses [14,107-108,117]. All of the absorption peaks corresponded to that of Carnall's conversion as $^4I_{15/2} \rightarrow {}^2G_{9/2}$ (365 nm), $^4G_{11/2}$ (377 nm), $^2H_{9/2}$ (406 nm), $^4F_{5/2}+{}^4F_{3/2}$ (450 nm), $^4F_{7/2}$ (488 nm), $^2H_{11/2}$ (521 nm), $^4S_{3/2}$ (544 nm), $^4F_{9/2}$ (651 nm), $^4I_{9/2}$(799 nm) and $^4I_{11/2}$ (978 nm) [10] . This indicate that the laser active Er^{3+} ions have entered into the (K,Na)NbO_3 crystalline phase. Similar results were reported recently [88,118]. This result is similar to glass 1.0 mol% of Er_2O_3 doped glass showed in Fig. 4.32.

When comparing the absorption coefficient with heat treatment temperature as showed in Fig. 4.38 and 4.39. It can be clearly seen that the heat treatment temperature played a significant role in control the ability of transmission. In Fig. 4.32, glass with 1.0 mol% of Er_2O_3 showed high absorption at glass with lowest treated temperature. This might become of the phase separation occurred inside the glass matrix.

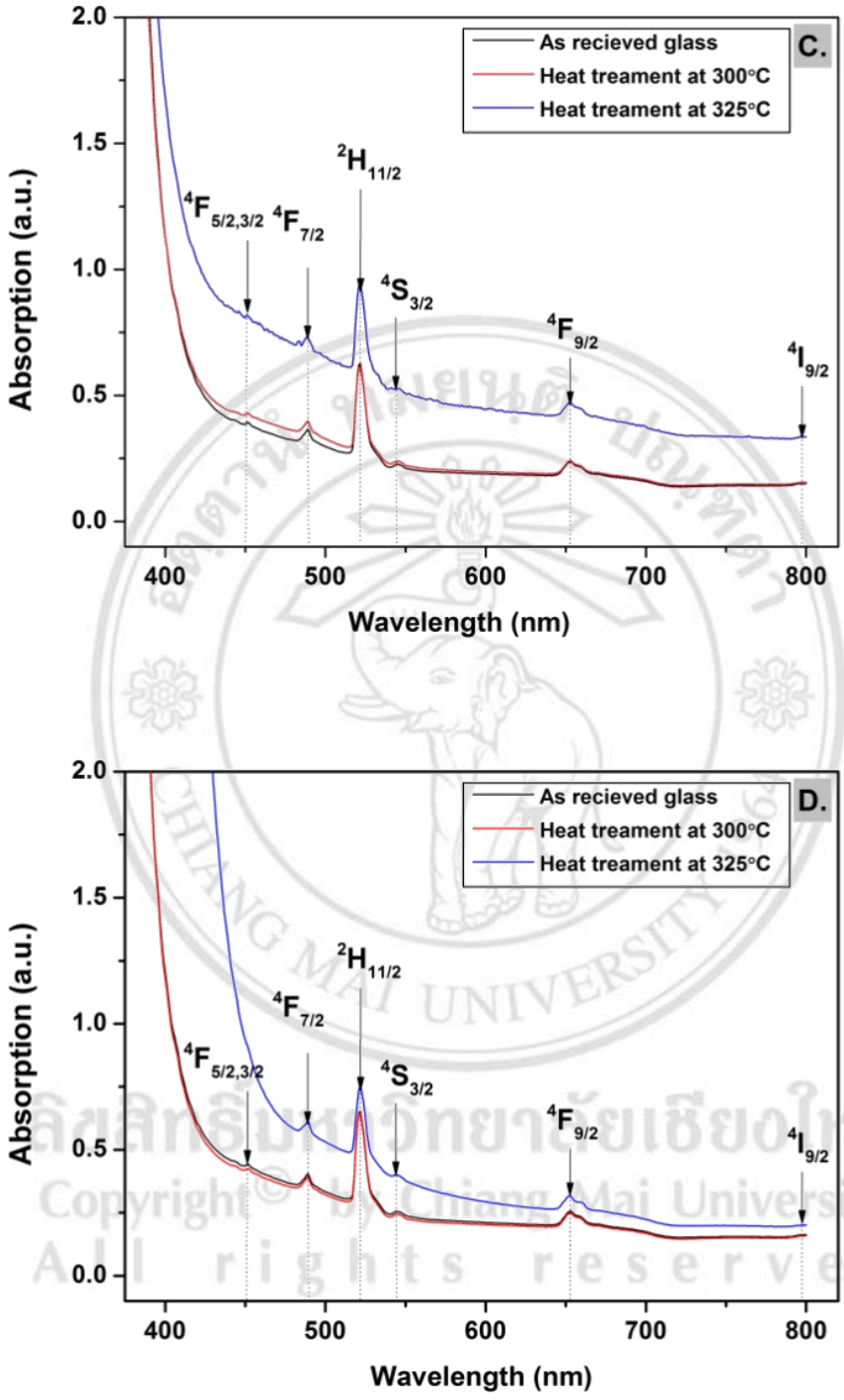

Figure 4.31 Absorbance spectra of glass ceramics 30KNN-70TeO_2 doped with 0.5 mol% Er_2O_3 in system C. and D. after heat treatment at different temperatures.

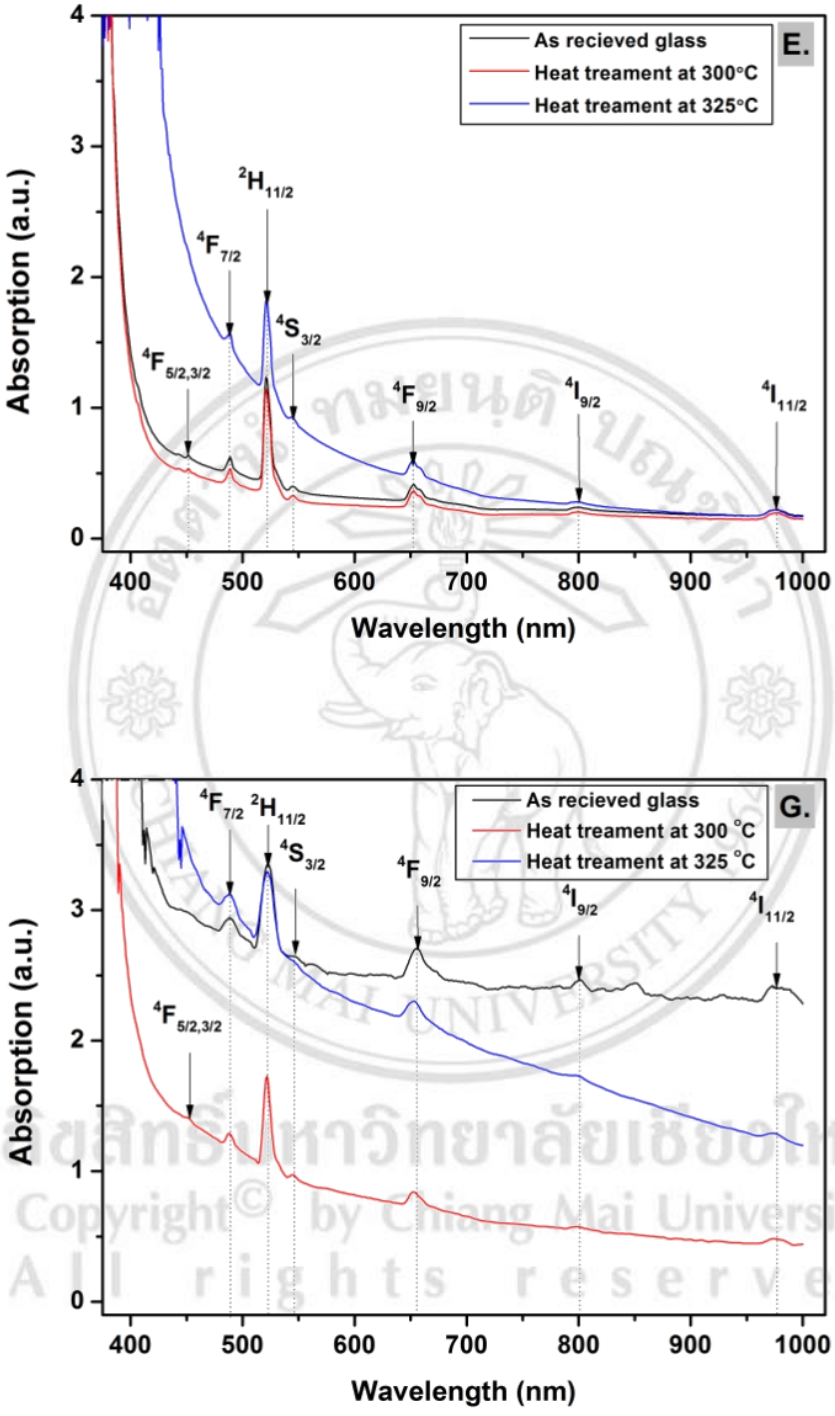

Figure 4.32 Absorbance spectra of glass ceramics 30KNN-70TeO_2 doped with 1.0 mol% Er_2O_3 in system E. and G. after heat treatment at different temperatures.

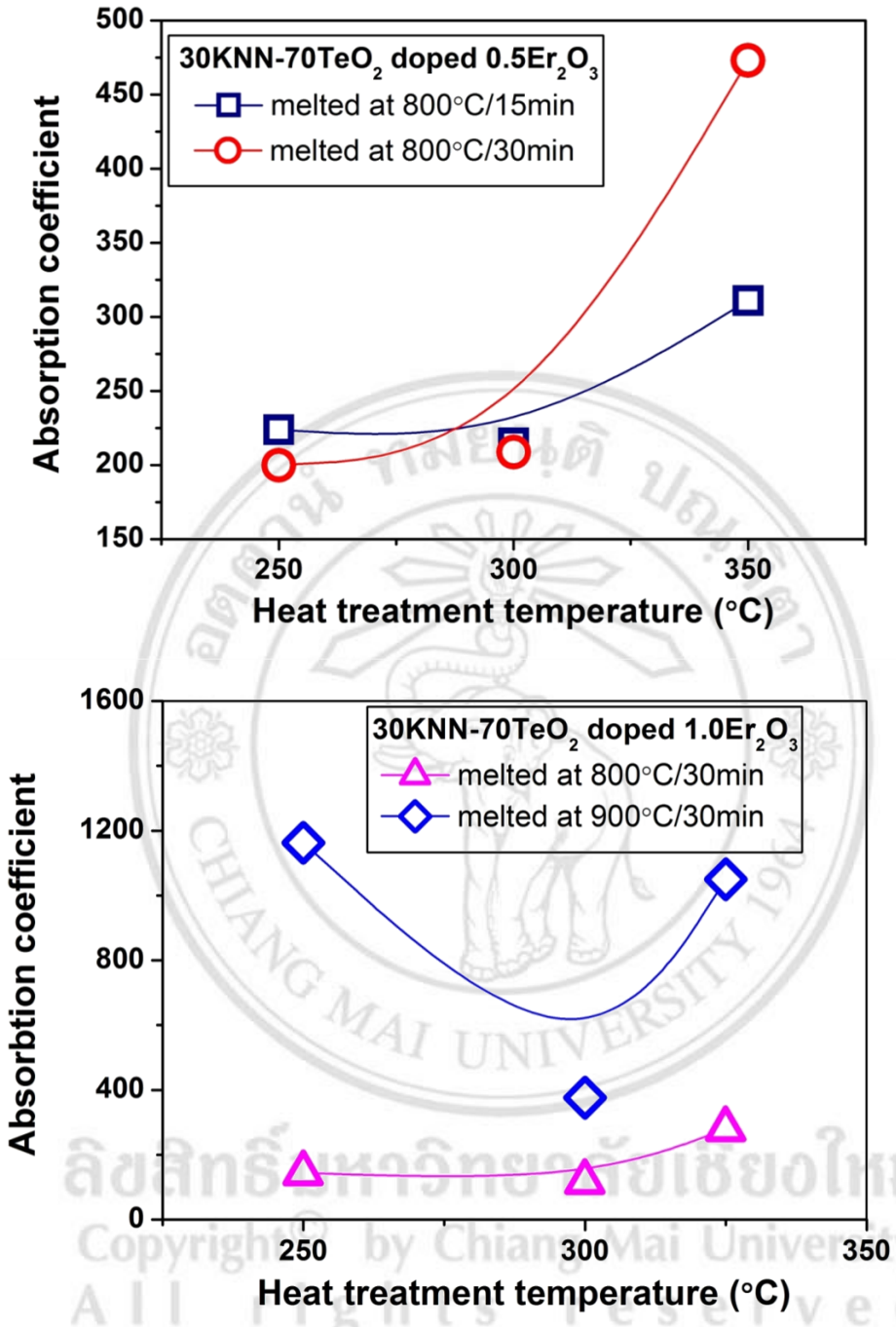

Figure 4.33 The absorption coefficient comparing with heat treatment temperature of 30KNN-70TeO2 doped 0.5 mol% and 1.0 mol% of Er_2O_3.

2) Refractive index and Energy band gap

Refractive index (n) and Energy band gap from the transmission cut-off wavelength (E_g) was shown in Table 4.6. The refractive index of all glasses are lying between 2.00 – 2.15. The optical band gap was

obtained by plotting $(\alpha hv)^2$ versus hv (where α is the absorption coefficient and hv is the photon energy), which is described by equation 4.3. The absorption coefficient α is obtained from Beer's law equation 4.4. The optical band gap, E_g of selected glass and glass-ceramics, varied between 2.45 and 3.20 eV, as showed in Fig. 4.34 and 4.35 and listed in Table 4.6.

Table 4.6 Refractive index and energy band gap of each glass composition.

Melting temperature (°C/min)	**Heat treatment Temperature (°C)**	**Refractive index (n) (532 nm.)**	**Energy band gap (Eg; eV)**
30KNN-70TeO_2 doped 0.5 Er_2O_3			
(C.) 800°C/ 15 min	As-received	2.07	3.06
	300	2.06	3.06
	350	2.05	2.96
(D.) 800°C/ 30 min	As-received	2.06	3.07
	300	2.05	3.07
	350	2.00	2.79
30KNN-70TeO_2 doped 1.0 Er_2O_3			
(E.) 800°C/ 30 min	As-received	2.09	3.15
	300	2.10	3.13
	325	2.15	2.74
(G.) 900°C/ 30 min	As-received	2.09	3.09
	300	2.15	2.88
	325	-	2.45

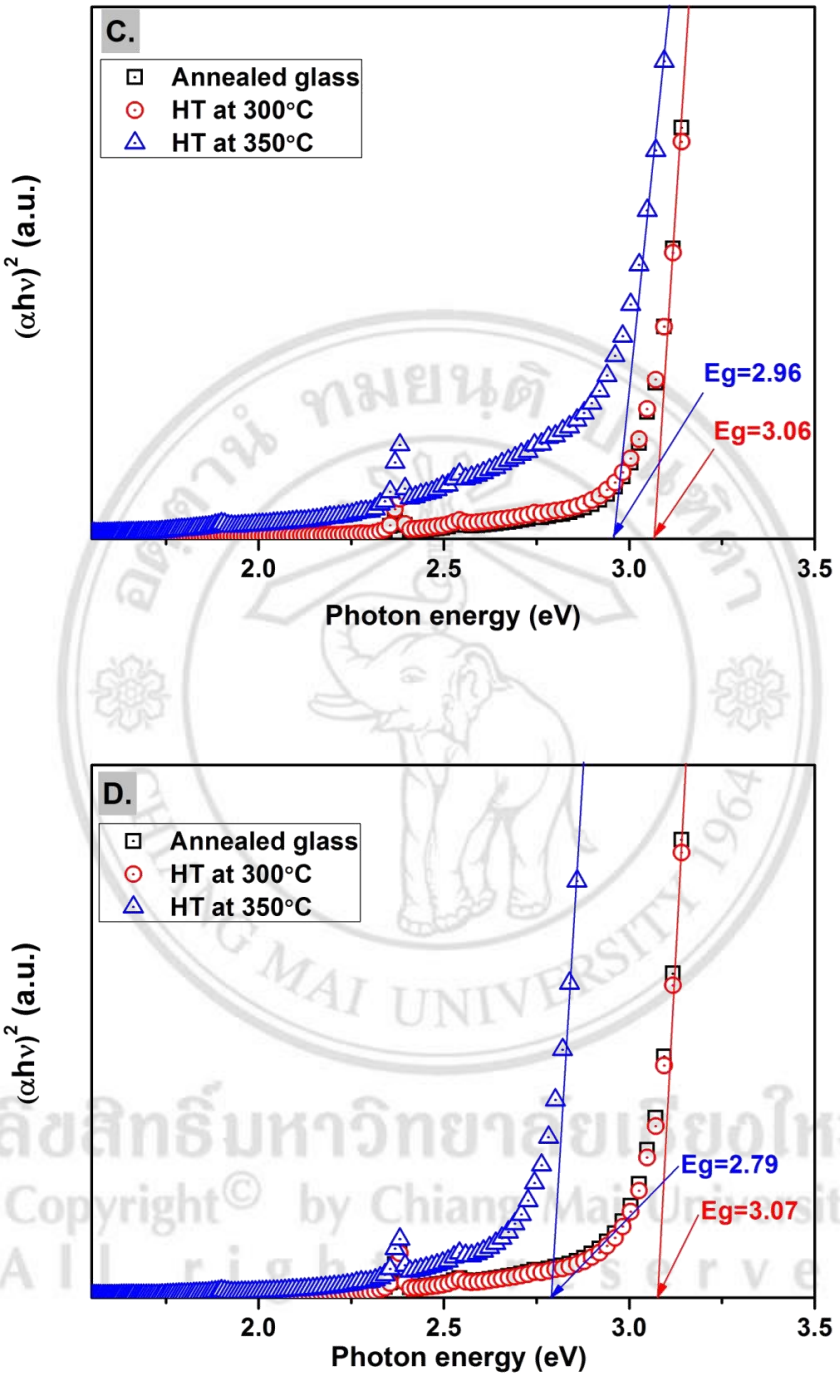

Figure 4.34 Photo energy of glass ceramics 30KNN-70TeO_2 doped with 0.5 mol% Er_2O_3 in system C. and D. after heat treatment at different temperatures.

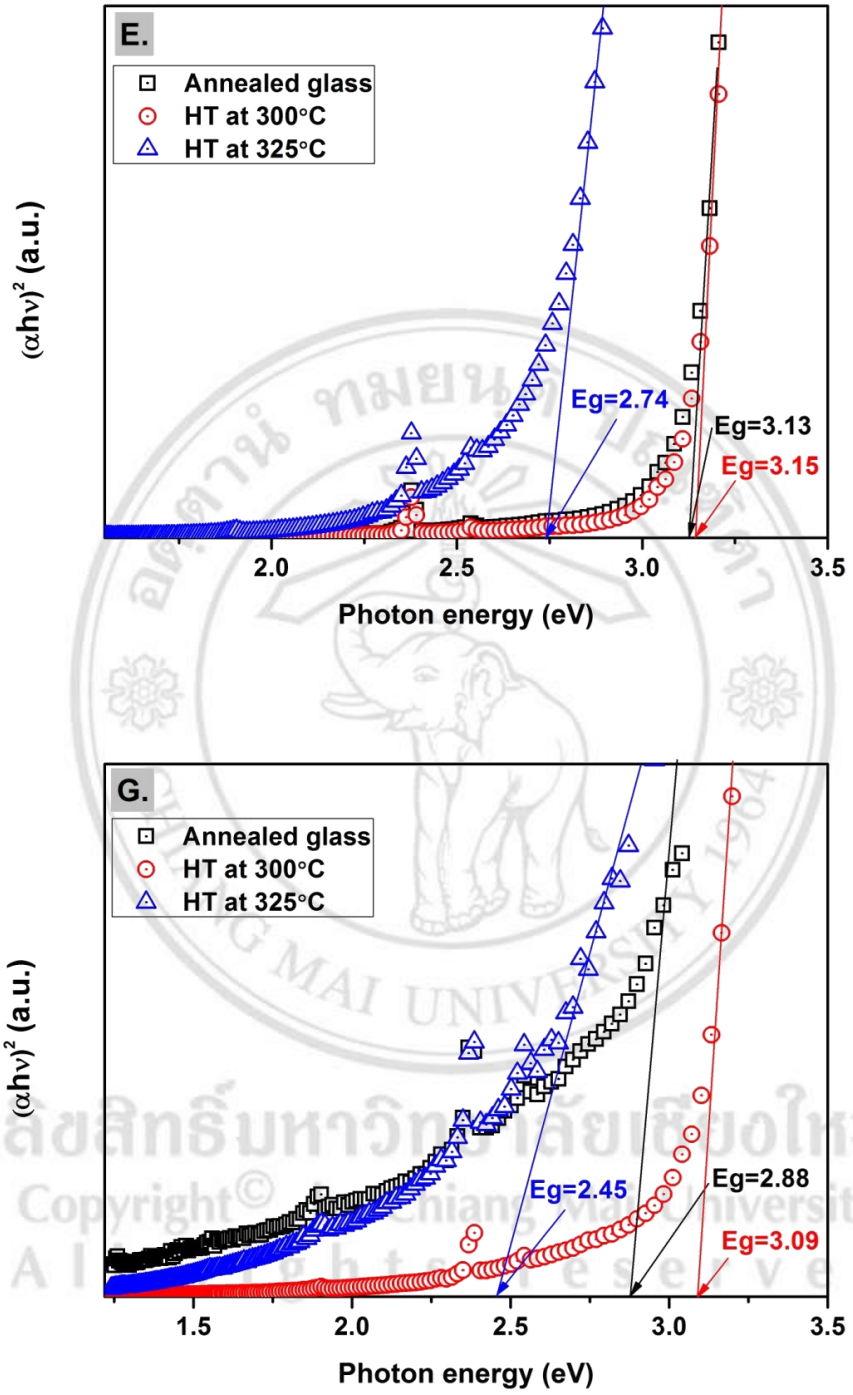

Figure 4.35 Photo energy of glass ceramics 30KNN-70TeO_2 doped with 1.0 mol% Er_2O_3 in system E. and G. after heat treatment at different temperatures.

3) Photoluminescence

The photoluminescence of 30KNN-70TeO_2 doped with 0.5-1.0 mol% of Er_2O_3 are showed in Figure 4.36 and 4.37, respectively. As-received glass was used to study the respond of LED light source excitation in wavelength of 345 nm. Glass doped 0.5 mol% Er_2O_3 exhibited 2 intense luminescence peak at 386 nm (purple) and 481 nm. (blue-green) While, the increasing of melting temperature cause the small shifting of peak, indicated that the melting temperature about 800°C -900°C showed no significant to the luminescence of glass. However, glass doped 1.0 mol% of Er_2O_3 was different in pattern.

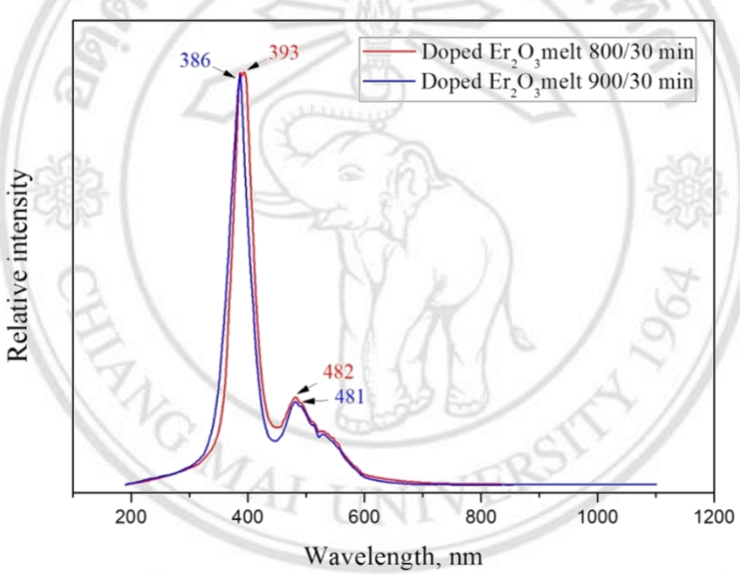

Figure 4.36 Photoluminescence patterns of glass 30KNN-70TeO_2 doped with 0.5 mol% Er_2O_3 samples in system C. and D.

After applied 345 nm LED light source to glass 30KNN-70TeO2 doped with 1.0 mol% of Er_2O_3, the broad intense peak at 500 nm (Green) is showed up. The different in the luminescence respond of 1.0 mol% dopant sample, might become from the high contents of Er_2O_3 ions. This is made Er ions also had high probability to entered crystal structure in glass-ceramics site.

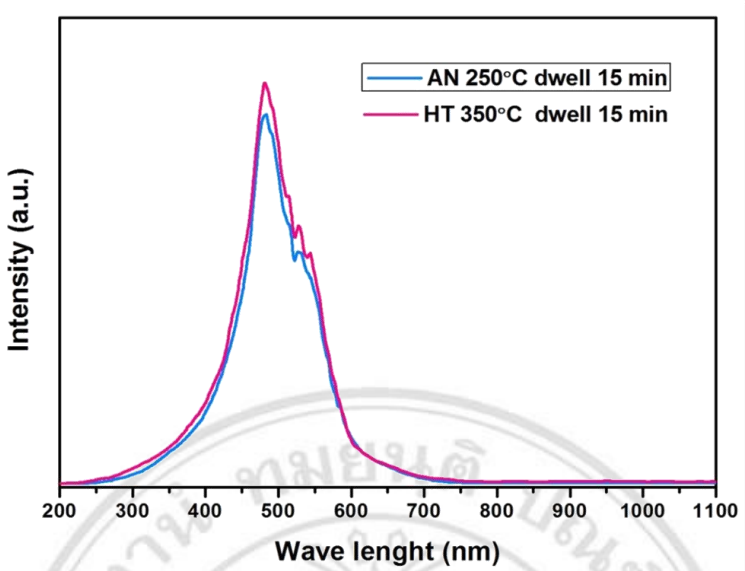

Figure 4.37 Photoluminescence patterns of glass 30KNN-70TeO_2 doped with 1.0 mol% Er_2O_3 in system E. and G.

4.2.7 Conclusion

The ferroelectric glass-ceramics from KNN-TeO_2 doped Er_2O_3 system have been successfully prepared via the incorporation method. The melting temperature and dwell time did not played a significant role for the type of crystalline phase in the glass ceramics. Dielectric properties of these glasses and glass-ceramics are high compared with another KNN containing glass-ceramic system. By the way, these glass ceramics possesses poor mechanical robust and low transparency. The more detail studies in terms of mechanical and optical properties, therefore, are needed in future works